Journal Pre-proof

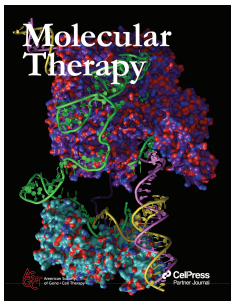

Repurposing base editors for targeted knock-in and simultaneous multiplex knockouts to generate allo-CAR T cells with minimal translocations

Glaser. Viktor, Becker. Lily Jo, Fuster-García. Carla, Aird. Eric Jackson, Huth. Luis, Nitulescu. Ana-Maria, Pu. Yaolin, Kassing. Isabell, Hartmann. Laura Marie, Flugel. Christian Luca, Kārkliņš. Roberts, Shaji Shona, Pouzolles. Marie, Stein. Maik, Andrieux. Geoffroy, Corn. Jacob Ellery, Cathomen. Toni, Volk. Hans-Dieter, Reinke. Petra, Kath. Jonas, Wagner. Dimitrios Laurin

PII: S1525-0016(26)00602-7

DOI: https://doi.org/10.1016/j.ymthe.2026.07.034

Reference: YMTHE 7640

To appear in: *Molecular Therapy*

Received Date: 16 September 2025

Accepted Date: 15 July 2026

Please cite this article as: Viktor G, Jo BL, Carla F-G, Jackson AE, Luis H, Ana-Maria N, Yaolin P, Isabell K, Marie HL, Luca FC, Roberts K, Shona S, Marie P, Maik S, Geoffroy A, Ellery CJ, Toni C, Hans-Dieter V, Petra R, Jonas K, Laurin WD, Repurposing base editors for targeted knock-in and simultaneous multiplex knockouts to generate allo-CAR T cells with minimal translocations, *Molecular Therapy* (2026), doi: https://doi.org/10.1016/j.ymthe.2026.07.034.

BERI

Base editor-mediated knock-in

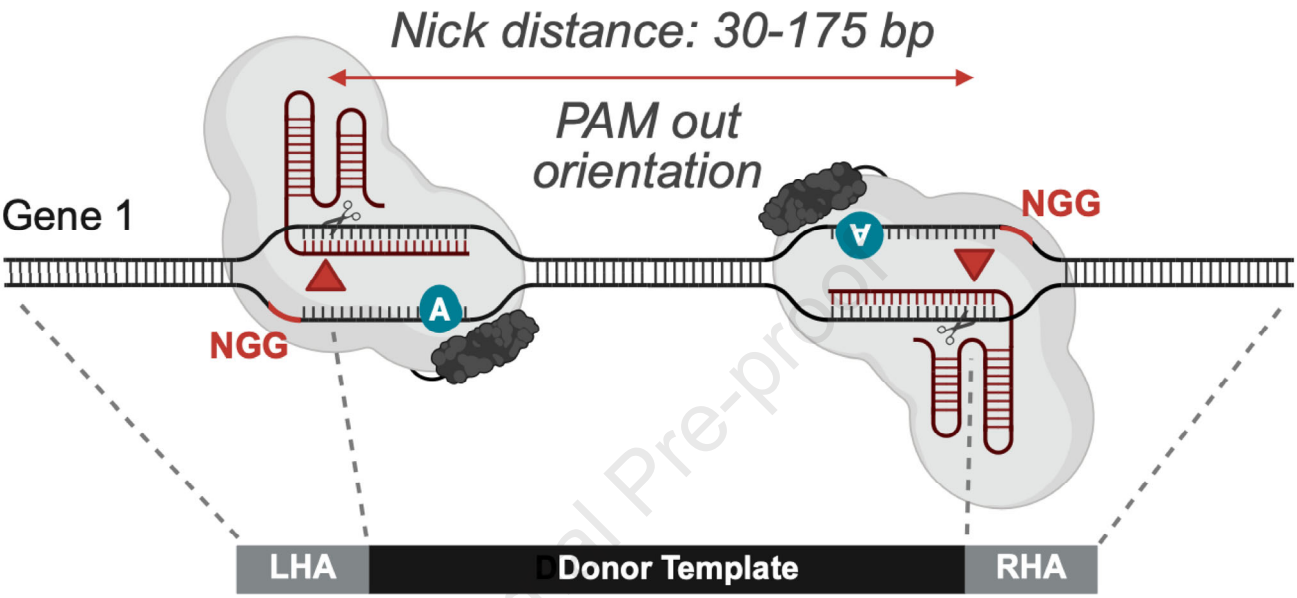

+

Base editor-mediated knock-outs for **MULTIPLEX EDITING**

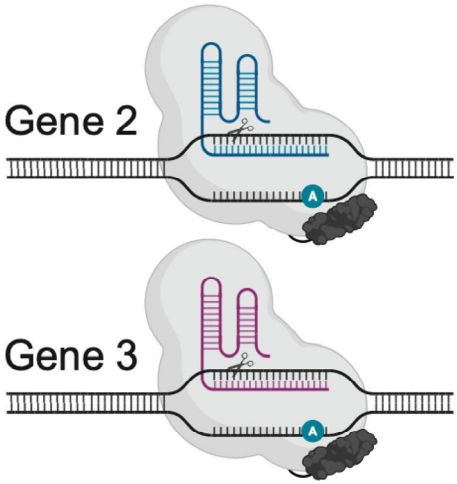

- highly efficient
- minimal translocations
- up to eleven edits

Repurposing base editors for targeted knock-in and simultaneous multiplex knockouts to generate allo-CAR T cells with minimal translocations

Glaser, Viktor (1,2,3); Becker, Lily Jo (1,2,3); Fuster-García, Carla (4,5); Aird, Eric Jackson (6); Huth, Luis (1,2,3); Nitulescu, Ana-Maria (1,2,3); Pu, Yaolin (1,2,3); Kassing, Isabell (1,2,3); Hartmann, Laura Marie (1,2,3,8); Flugel, Christian Luca (1,2,3), Kārkliņš, Roberts (3,8); Shaji, Shona (8); Pouzolles, Marie (8); Stein, Maik (2); Andrieux, Geoffroy (7); Corn, Jacob Ellery (6); Cathomen, Toni (4,5); Volk, Hans-Dieter (3,9); Reinke, Petra (3,9); Kath, Jonas (1,2,3,8,#); Wagner, Dimitrios Laurin (1,2,3,8,10,11,#,*)

(1) Berlin Center for Advanced Therapies (BeCAT), Charité - Universitätsmedizin Berlin, 13353 Berlin, Germany
(2) BIH Center for Regenerative Therapies (BCRT), Berlin Institute of Health (BIH), 13353 Berlin, Germany
(3) Institute of Medical Immunology, Charité - Universitätsmedizin Berlin, 13353 Berlin, Germany
(4) Institute for Transfusion Medicine and Gene Therapy, Medical Center-University of Freiburg, 79106 Freiburg, Germany
(5) Center for Chronic Immunodeficiency, Faculty of Medicine, University of Freiburg, 79106 Freiburg, Germany
(6) Department of Biology, Institute of Molecular Health Sciences, ETH Zurich, 8093 Zurich, Switzerland
(7) Institute of Medical Bioinformatics and Systems Medicine, Medical Center-University of Freiburg, Faculty of Medicine, University of Freiburg, 79110 Freiburg, Germany

(8) Center for Cell and Gene Therapy, Baylor College of Medicine, Houston, 77030, United States of America

(9) Tcbalance Biopharmaceuticals GmbH, 13125 Berlin, Germany

(10) Department of Molecular and Cellular Biology, Baylor College of Medicine, Houston, 77030, Texas, United States of America

(11) Dan L. Duncan Comprehensive Cancer Center, Baylor College of Medicine, Houston, 77030, Texas, United States of America

# These authors contributed equally to this work

* Corresponding author: Dimitrios L. Wagner - dimitrios-l.wagner@charite.de

Abstract

Multiplex genome editing of cellular therapies frequently requires multiple DNA double-strand breaks (DSBs), which can induce genotoxicity through chromosomal rearrangements and large deletions. Base editors enable targeted sequence changes with minimal DSBs and are widely used for gene disruption, but their capacity for transgene insertion has remained unexplored. Here, we developed base editor–mediated knock-in (BEKI), a non-viral platform combining transgene insertion with multiplex gene disruption using a single enzyme. BEKI repurposes the base editor's Cas9 nickase domain to generate paired nicks (inducing a localized DSB) at the knock-in locus, while achieving multiplex knockouts through base editing. Optimized guide RNA orientation and spacing enabled efficient transgene insertion across multiple T cell-relevant genomic loci. DNA-PK inhibition enhanced knock-in efficiency but increased kilobase-scale deletions, which were mitigated by co-inhibition of Polθ. Compared with multiplex Cas9 editing, BEKI markedly reduced chromosomal translocations while preserving cell viability. BEKI supported targeted CAR knock-in alongside up to 10 simultaneous gene knockouts, enabling the generation of allogeneic CAR T cells with enhanced cytokine secretion and resistance to immunosuppressants and allo-rejection. Together, BEKI provides a streamlined and scalable strategy for multiplex CAR T-cell engineering with improved genomic stability, advancing safer next-generation cell therapies for cancer and autoimmune diseases.

Introduction

Recent advances in CRISPR-Cas-based gene editing have transformed cell and gene therapies by enabling programmable, site-specific modifications. Conventional Cas-endonucleases, such as *Streptococcus pyogenes* Cas9 (SpCas9) and *Acidaminococcus sp.* (AsCas12a), introduce DNA double-strand breaks (DSBs), which are repaired by endogenous DNA repair mechanisms. The non-homologous end joining (NHEJ) pathway rapidly ligates the DNA ends and often introduces small insertions or deletions (indels), which can be used for targeted gene knockout (KO). In contrast, homology-directed repair (HDR) leverages a homologous DNA template to achieve precise repair. By supplying an exogenous template, HDR can be harnessed for targeted transgene integration, commonly referred to as knock-in (KI). Leveraging these major DNA repair mechanisms enables precise engineering of cell therapies.

CRISPR-Cas-assisted HDR allows the non-viral generation of chimeric antigen receptor (CAR) T cells with controlled expression, for instance by integrating the CAR construct into defined genomic loci such as the *T cell receptor alpha constant* (*TRAC*) or *CD3ζ* gene, thereby eliminating the need for exogenous promoters[1–4]. Compared to virally transduced CAR T cells, characterized by random integration and exogenous promoter–driven expression, *TRAC*- and *CD3ζ*-integrated CAR T cells display reduced exhaustion and improved functionality[3,5]. Moreover, CRISPR KI at these loci disrupts the T cell receptor (TCR) complex, preventing graft-versus-host disease (GvHD) and forming the foundation of allogeneic CAR T cell therapies[6,7]. While non-virally engineered allogeneic CAR T cells promise scalable, off-the-shelf therapies derived from healthy donors at reduced cost[8], they must be further engineered to evade rejection by the host's immune system. This can be achieved by disrupting the

genes *beta-2-microglobulin* (*B2M)* and *class II major histocompatibility complex transactivator* (*CIITA*) to abrogate human leukocyte antigen (HLA) class I and II expression, respectively, and by introducing inhibitory receptors such as HLA-E to suppress NK cell-mediated rejection[9–11].

Allogeneic CAR T cells may benefit from additional gene edits (such as KOs), including previously described strategies to prevent T cell exhaustion[12] and improve function within the immunosuppressive tumor microenvironment[13]. Gene editing can also render CAR T cells resistant to immunosuppressive drugs. For example, KO of *FK506-binding protein 12* (*FKBP12*) confers resistance to tacrolimus and rapamycin[14], and may thus enable treatment of patients who require systemic immunosuppression. Beyond these rational KO approaches, genome-wide CRISPR KO screens have been employed to uncover genes whose deletion can overcome CAR T cell dysfunction and improve long-term functionality[15–20]. One of the hits, KO of *RAS p21 protein activator 2* (*RASA2*), exhibited enhanced persistence and effector functions[21]. Although promising on their own, these edits gain full relevance in combination, especially for allogeneic CAR T cells, where multiplex engineering is likely essential for durable responses.

During multiplex editing with conventional Cas endonucleases, the simultaneous induction of multiple DSBs carries a high risk of genotoxicity, giving rise to structural variants (SVs) such as large deletions[22], chromosome truncations[23], chromosome loss[24] and translocations, at both on-target and off-target sites[25], potentially causing unintended gene fusions. While specific events from multiplex editing have not been linked to oncogenesis, certain recurrent translocations and fusions are established drivers of oncogenesis[26]. Given these concerns, mitigating genotoxicity is a critical consideration in the development of next-generation cellular therapies. Adenine base

editors (ABEs) and cytosine base editors (CBEs) offer an alternative by employing a SpCas9 nickase (nCas9) fused to a deaminase to introduce predictable base substitutions without generating DSBs[27,28]. CBEs can introduce premature stop codons, while both ABEs and CBEs can disrupt splice sites to achieve efficient gene KO[29–31].

Here, we introduce **b**ase **e**ditor-mediated **k**nock-**i**n (BEKI), a strategy that repurposes the D10A nCas9-domain of base editors for double nick-mediated HDR, while enabling multiplex-editing with minimal translocations. We explored BEKI in four loci relevant to T cell engineering – *TRAC, CD3ζ, CD3ε*, and *B2M* – systematically assessing the impact of sgRNA design on editing efficiency. To further improve transgene insertion efficiency, we harnessed DNA repair modulation using small molecule inhibitors, previously used to enhance Cas9-based gene editing[32,33]. Using on-target long-read Nanopore sequencing, we examined genomic integrity following editing, and found that DNA-PK inhibition increased kilobase-scale deletions, an effect that was mitigated by co-inhibition of Polθ. Utilizing the inherent base editing ability, BEKI enabled multiplex gene disruption by targeted splice site disruption. BEKI CAR T cells with dual knockout were assessed for translocation frequencies using CAST-Seq and ddPCR, revealing minimal chromosomal translocations compared with multiplex Cas9-edited T cells. We generated BEKI CAR T cells with five edits introduced in parallel: *TRAC* KI of a CAR, and KOs of *B2M*, *CIITA*, *RASA2*, and *FKBP12*, conferring TCR replacement, immune evasion, enhanced cytokine production, and resistance to immunosuppressive drugs. Finally, we demonstrated the generation of BEKI CAR T cells with up to 10 additional simultaneous KOs of relevant genes for T cell engineering. This study establishes BEKI as a versatile platform for generating multiplex-engineered allogeneic CAR T

cells by expanding the capability of base editors from precise single-base edits to simultaneous double nick-mediated insertion of therapeutic transgenes.

Results

Repurposing the D10A nCas9 domain of base editors enables site-specific double nick-mediated integration of CAR transgenes

Previous studies using D10A nCas9 for double nicking have described that PAM orientation and the distance between nicks critically influence both HDR and NHEJ frequencies[34–36]. To develop an efficient double nick-mediated KI strategy, we designed 12 single-guide RNAs (sgRNAs) targeting the *TRAC* locus for in-frame insertion of a second generation CD19-specific CAR transgene (**Fig. 1A**). Specifically, 6 sgRNAs targeting the sense strand were combined with 6 sgRNAs targeting the antisense strand, creating a matrix of 36 distinct sgRNA combinations. The resulting sgRNA pairs varied in distance between the nick sites and exhibited either PAM-in or PAM-out orientation (**Fig. 1B)**. We electroporated activated primary human T cells with mRNA encoding a D10A nickase SpCas9[37], two synthetic sgRNAs targeting opposed DNA strands and a linear double-stranded HDR donor template containing homology arms matching the genomic regions flanking the nick sites[36]. Among all sgRNA combinations tested, T1+T7 yielded the highest efficiency, with a mean of 27.5% CAR^+ cells as measured by flow cytometry (**Fig. 1C)**. Notably, efficient editing outcomes with >10% CAR^+ cells were only achieved using sgRNA combinations with a PAM-out orientation and a minimum distance of 30 bp between nicks (**Fig. 1C)**, aligning with previous nCas9-mediated KI studies in cell lines[34,35]. To test the proposed concept of BEKI, we replaced the nCas9 mRNA with ABE mRNA, achieving CAR integration rates of up to 16.0% (T1+T9) (**Fig. 1D**). Utilizing CBE for BEKI of a CAR yielded up to 9.0% of CAR+ cells (T2+T8) (**Fig. 1E**). While base editors can be repurposed for efficient double nick-mediated transgene insertion, fewer sgRNA combinations resulted in efficient KI compared to editing with nCas9 (**Fig. 1C-E**). Notably, we observed

relatively higher CD3 KO efficiencies with BEKI compared to nCas9 editing in T cells transfected with sgRNA T4 targeting a splice site (**Fig. S1)**. sgRNA pairs that enable robust nCas9 activity do not necessarily yield high BEKI efficiency (**Fig.1 C-E, Fig. S2**). Further, BEKI using ABE or CBE generally resulted in lower KI-efficiencies compared to nCas9, while we did not observe a clear impact of the number of target nucleotides in the base editing window on BEKI rates (**Fig. S3**).

BEKI enables efficient gene editing at multiple therapeutically relevant loci

To further validate BEKI using ABE, we tested three previously described KI strategies at loci relevant for T cell engineering: (1) CD19-CAR insertion into *CD3ζ* exon 2 using a truncated CAR (*trunc*CAR) to leverage the genomic *CD3ζ* locus for CAR signaling and transcript termination[3], (2) HLA-E insertion into *B2M* exon 2 (to evade NK-mediated rejection)[11], and (3) CD19-scFv insertion into *CD3ε* exon 3 creating a T cell receptor fusion construct (TRuC)[38] (**Fig. 2A-C**). Based on results from targeting the *TRAC* locus, we performed a less extensive sgRNA screening for these novel BEKI strategies, excluding sgRNA pairs with PAM-in orientation. BEKI edited cells were analyzed by flow cytometry to detect expression of the transgenic receptors (**Fig. S4**). We achieved relatively high KI-efficiencies across all three loci, especially using the sgRNA combinations Z4+Z6/Z7 (*CD3ζ*, 13.5%/12.4%), B2+B5/B4+B6 (*B2M*, 10.6%/9.2%) and E1+E4 (*CD3ε*, 10.3%) (**Fig. 2A-C**). Certain sgRNAs such as B4 targeting a splice sites in the *B2M* gene (published by Gaudelli *et al*.[39]) resulted in highly efficient KO (**Fig. S5A**). The sgRNA pairs that yielded high KI-rates generally also induced efficient gene disruption at the target loci with KO rates of 61%, 77%, 67% and 48% for the *TRAC, CD3ζ, B2M* and *CD3ε* loci, respectively (T1+T9, Z4+Z7, B4+B6, E3 + E4; **Fig. S1B & S5B**). For *B2M*, the combination of B4+B6 was selected for following experiments, considering both high HLA-E KI and *B2M* KO frequencies

(**Fig. S5B**). In general, we observed a trend of decreasing KI rates with increasing distances between the nicks (**Fig. 2D**). Interestingly, the presence of adenines within the base editing window defined by the sgRNAs used did not appear to markedly affect KI frequencies (**Fig. 2E-F**). To sum up, efficient BEKI strategies could be established at all tested loci; and we conclude that optimal design requires sgRNA pairs with PAM-out orientation and nick distances between ~30 to 175 bp.

HDR enhancers improve BEKI efficiency and enable potent in vivo activity of CD19-CAR T cells

We and others have shown that selective inhibition of competing DNA repair pathways promotes HDR, thereby enhancing insertion of therapeutically relevant transgenes[4,40]. Based on this, we tested various NHEJ inhibitors for their effect on BEKI-mediated CAR insertion into *CD3ζ*, with the DNA-PK inhibitors nedisertib (M3814) and AZD7648 showing the strongest enhancement (**Fig. S6A**). Combining AZD7648 with Polθ inhibitors further improved insertion efficiencies across all tested sgRNA combinations compared to untreated controls, achieving KI frequencies of up to 40.2% (Z4+Z7, **Fig. 3A**). We titrated the concentration of AZD7648 in the presence of the Polθ inhibitor ART558 and identified 0.375 µM of AZD7648 as the optimal concentration for KI efficiency (**Fig. S7**). DNA-PK and Polθ inhibition also effectively improved CBE-mediated CAR insertion (**Fig. 3B).** Using the most effective sgRNA combinations at the *TRAC*, *CD3ζ*, *B2M*, and *CD3ε* loci, DNA-PK and Polθ inhibitor treatment resulted in an average 2.7-fold increase in ABE-mediated KI efficiency across all four targets (**Fig. S6B**). We then evaluated the antitumor efficacy of BEKI-engineered *CD3ζ*-CAR T cells generated with DNA-PK and Polθ inhibitors in a xenograft model of acute lymphoblastic leukemia. Immunodeficient mice received 0.5 × 10^6 luciferase-labeled $CD19^+$ Nalm-6 cells intravenously, followed 7 days later by infusion of 0.5 × 10^6 CAR^+

cryopreserved T cells (**Fig. 3C**). *In vivo* bioluminescence imaging showed significantly reduced tumor growth in mice treated with *CD3ζ*-CAR T cells compared with mice receiving TCR/CD3-negative (*TRAC* KO) control T cells. (**Fig. 3C**). Consistently, 28 days post leukemia inoculation, leukemia cells were undetectable in blood from *CD3ζ*-CAR-treated mice (0/5) but detectable in 4/5 controls (**Fig. 3C**).

AZD7648-induced large deletions can be limited by co-treatment with ART558 and the DNA template

We assessed on-target gene editing outcomes of *TRAC* CAR T cells by performing a PCR followed by long-read sequencing using Oxford Nanopore Technologies (ONT) (**Fig. 4A**). The unedited amplicon measured 4.4 kb, whereas integration of the 2 kb CD19 CAR resulted in reads of approximately 6.4 kb, while shorter reads (<4.4 kb) were indicative of deletions. Quantifying the reads with deletions over 2 kb and 1 kb revealed an increase in deletion frequency for AZD7648 treated samples independent of the editing enzyme (Cas9, Cas12a, ABE) (**Fig. 4B, C; Fig. S8A, B**). Additionally, including the Polθ inhibitor ART558 minimized kilobase scale deletions (**Fig. 4B, C**). To investigate the frequency of megabase scale deletions we quantified copy number fold changes using a ddPCR assay targeting the *ZFHX2* gene, located approximately 1 Mb from the *TRAC* gene on chromosome 14, relative to *KM2TC* on chromosome 7 (**Fig. 4D**). When performing the assay with Cas9-treated cells in the absence of donor DNA template, we observed low mb scale deletion frequencies, which slightly increased under AZD7648 treatment (**Fig. 4E)**. Compared to this positive control we did not observe a decrease in average fold change for Cas9, Cas12a or ABE treated samples when using a DNA template irrespective of the enhancer used (**Fig. 4F, Fig. S8C**).

Multiplex base editing enhances BEKI CAR T cell function in the presence of immunosuppressants facilitating allogeneic applications

Leveraging the inherent base editing capability of the BEKI platform for simultaneous transgene KI and multiple base edits, we aimed to enhance *TRAC*-CAR T cells by introducing additional KOs of *RASA2*[21] and *FKBP12*[14]. ABE-mediated splice site disruption of *FKBP12* conferred resistance to the calcineurin inhibitor tacrolimus, as indicated by sustained cytokine production in its presence (**Fig. S9A**). Efficient splice site disruption of *RASA2* enhanced cytokine production upon polyclonal activation (**Fig. S9B**). Although *RASA2* KO has previously been linked to enhanced proliferation and cytotoxicity in immunosuppressive environments, such as during tacrolimus treatment[21], *RASA2* base editing alone did not sufficiently restore cytokine production under tacrolimus exposure in our hands (**Fig. S9C**). Consequently, we compared two strategies for combining CAR KI with disruption of both ***R****ASA2* and ***F****KBP12* (CAR + *RF* KO): (1) BEKI, in which the ABE mediated both CAR KI and the KOs, and (2) a control approach with Cas12a-mediated CAR KI with ABE-mediated KOs. Both strategies successfully enabled tumor-specific cytokine production in the presence of tacrolimus (**Fig. S9C**). Next, we successfully generated quintuple-edited BEKI CAR T cells combining *TRAC*-CAR KI with four base editor-mediated KOs of ***B****2M*, ***C****IITA,* ***R****ASA2* and ***F****KBP12* (CAR + *BCRF* KO) (**Fig. S10A**). Importantly, the addition of two or four sgRNAs for splice site disruption did not compromise CAR KI rates, while reaching high KO efficiencies for HLA class I and II (**Fig. S10B**). Interestingly the CAR+ cells were largely negative for the additional KO targets (**Fig. S10C, D**). Viability was comparable across all BEKI-edited groups, whereas conventionally multiplexed Cas9-edited samples exhibited markedly reduced viability following treatment with DNA-PK and Polθ inhibitors (**Fig. S10E**). Quintuple-edited CAR T cells showed comparable expansion and CD4:CD8 ratios to single- and dual-edited cells. Across all conditions,

edited CAR T cell products retained a predominantly naïve-like phenotype; however, inclusion of *RASA2* KO was associated with slightly increased differentiation among $CD8^+$ CAR^+ T cells (**Fig. S10F**). The quintuple-edited BEKI CAR T cells evaded allo-specific T cell cytotoxicity (**Fig. S11A**) and maintained CAR function under therapeutic rapamycin concentrations (**Fig. S11B**), supporting their use in allogeneic settings and in patients receiving immunosuppressive therapy.

BEKI minimizes chromosomal translocations during simultaneous KI and multi-gene KO

Aiming to benchmark translocation risk, we compared BEKI against two other multiplex strategies for generating ***T****TRAC*-CAR T cells in combination with ***R****ASA2* and ***F****KBP12* KOs (CAR + TRF KO): (1) Cas9 for CAR KI and the additional KOs, expected to induce translocations between the on-target DSBs, and (2) Cas12a for CAR KI plus ABE for the KOs, previously shown not to induce translocations[41]. As a positive control for inducing translocations, we included Cas9-mediated triple KO without an HDR template (KO only) (**Fig. 5A**). Cas12a + ABE achieved the highest CAR integration frequencies, whereas BEKI matched Cas9 in KI efficiency but with lower CD3 KO frequencies; *RASA2* and *FKBP12* KOs, however, were most efficient with ABE (**Fig. 5B**). Expansion rates were similar between the different samples with slightly lower cell numbers for Cas9-treated conditions on d14 (**Fig. S12**). To avoid interference with the HDR template, we assessed genomic integrity by CAST-Seq with the KO-only samples (**Fig. 5C**). The KO-only samples showed similar KO frequencies comparable to those observed in the presence of the DNA template (**Fig. S13A**). CAST-Seq identified several types of genomic alterations: large chromosomal aberrations at the *TRAC* target site (**Fig. S13B**), translocations between *TRAC* and the two other on-target loci (*FKBP12* and *RASA2*), as well as off-target–mediated

translocations (OMTs) (**Fig. 5C**). Chromosomal rearrangements between *TRAC*, *RASA2*, and *FKBP12* were detected with all strategies (**Fig. 5C**). Furthermore, while OMTs were frequent with Cas9 multiplex editing, only one was detected with Cas12a + ABE, and none with ABE (BEKI) (**Fig. 5C**). For samples treated with DNA-PK and Polθ inhibitors, we identified a higher number of OMTs in Cas9 multiplexed cells, whereas only two OMTs were detected for Cas12a + ABE (BEKI), which were of low frequency compared to some OMTs observed in the Cas9 condition with and without enhancer. (**Fig. 5D**). Most off-targets were associated with the *FKBP12* sgRNA and could likely be mitigated by selecting a more specific sgRNA (**Table S4**). We next quantified translocation frequencies by ddPCR, designing probes for all six possible balanced translocations between *TRAC*, *RASA2*, and *FKBP12*. These translocations were readily detected in Cas9-edited cells ((I) *TRF* KO, (II) CAR + *TRF* KO), with frequencies up to 4%, whereas such translocations were undetectable within the limit of detection of 0.03% by ddPCR in cells edited using either (III) Cas12a + ABE or (IV) multiplex BEKI, demonstrating their superiority in maintaining genomic integrity (**Fig. 5D, Table S5**).

BEKI enables efficient multiplexed editing for combining CAR KI with up to 10 KOs

To assess the extent to which additional KOs can be combined with BEKI, we targeted genes that could individually be beneficial for next-generation CAR T cell products. For this purpose, we stepwise added sgRNAs to BEKI-engineered CD3ζ-CAR T cells to disrupt *B2M, CIITA, CD54, CD58, CD38, CD2, CD5, CD7, Fas (CD95)*, and *CD45* (**Fig. 6A**). With increasing numbers of KOs, KI efficiency progressively decreased, reaching 19.4% of the KI-only condition when 10 additional KOs were introduced. In contrast, KO efficiencies were only modestly affected, remaining at an average of 79.7% of the single-KO frequencies (**Fig. 6, Fig. S14A–E**). While day 1 viability

declined with increasing editing complexity, no impairment in cell expansion was observed over a 14-day culture period (**Fig. S14F, G**). Comparable results were observed for KO-only controls lacking a DNA template, although KO frequencies were slightly lower in these conditions (**Fig. S15**). Notably, the resulting *CD3ζ*-CAR T cell population was negative for most KO targets, indicating relatively homogeneous editing outcomes. This observation prompted us to enrich CAR^+ cells by MACS-mediated depletion of residual CD3-positive cells. CD3 MACS depletion yielded a CD3-negative product with an increased CAR frequency and further enrichment of the additional KOs (**Fig. S16A-B**). To assess scalability in a clinically oriented manufacturing workflow, BEKI-edited CAR T cells were expanded in G-Rex bioreactors for 7 days and subjected to MACS depletion during the final production phase. Mean CAR^+ T cell yields reached 9-fold of input cell numbers despite expected MACS-associated cell loss (range: 6–13-fold), supporting the feasibility of achieving clinically relevant cell numbers. (**Fig. S16C**). Collectively, these findings establish BEKI as a scalable platform for the generation of highly multiplex-engineered next-generation T cell therapies.

Discussion

Here we show that base editors can be repurposed for targeted KIs. By exploiting their D10A nCas9 domain to induce double nicks and stimulate HDR, we extend their utility beyond single nucleotide editing. Coupling this KI capacity with their established ability to mediate gene KOs, BEKI enables complex engineering with a single enzyme. This approach effectively minimizes chromosomal translocations, a major drawback of conventional Cas9-based multiplex editing. To guide the design of new BEKI strategies, we note that, consistent with early nCas9-based double-nick approaches[34,35], efficient transgene KI was achieved when sgRNAs were selected in a PAM-out orientation creating nicks on opposite DNA strands at a distance of ~30 to 175 bp. Potential base editing mediated through the sgRNA pair used for double nicking had no evident impact on BEKI efficiency, likely due to the PAM-distal position of the catalyzed base substitution, a region where sgRNA mismatches are well tolerated by Cas9[42]. Notably, sgRNA screening identified distinct guide combinations that performed best for ABE- and CBE-based BEKI, suggesting that enzyme-specific editing dynamics influence optimal guide selection. In the case of CBEs, the fused uracil glycosylase inhibitor (UGI) present in the BE4 architecture may affect the efficiency of iterative nicking required for HDR. Selecting sgRNAs with minimal editable bases within the base editor activity window may help limit unintended base editing events that could reduce HDR efficiency. ABE-mediated BEKI achieved higher knock-in efficiencies than CBE-based BEKI in our system, consistent with observations from the accompanying study by Skeate *et al.*[43], and we therefore focused subsequent experiments on ABE-based strategies.

Using BEKI at the *TRAC* locus, we observed KO rates exceeding 60% with sgRNA pairs spaced up to 250 bp apart (**Fig. S1**), contrasting a previous report that increasing nick distance reduces NHEJ frequencies[36]. To achieve high KO rates, sgRNAs designed for base editing of splice sites were effectively repurposed for KI strategies (*TRAC* sgRNA T4, **Fig. S1,** *B2M* sgRNA B4 **Fig. S5**). Surprisingly, the *CD3ζ* targeting sgRNA Z3 caused high KO rates (**Fig. S5**), likely due to ABE induced amino acid changes (L34P/L35P) in the transmembrane domain of CD3ζ, potentially disrupting the α-helix structure of the transmembrane domain and disrupting TCR assembly[44]. These findings highlight the importance of considering potential amino acid-altering base edits introduced by the sgRNA pair used for double nicking.

At the 4 targeted loci, baseline KI efficiencies with BEKI were modest, averaging around 10% (**Fig. 1-2**), underscoring the need for strategies to increase editing rates to achieve clinically relevant cell yields. Pharmacologic inhibition of DNA-PK has been shown to increase KI rates but at the cost of promoting large deletions, while Polθ inhibition can counteract this undesired effect[4,32,33]. We applied the combination of DNA-PK and Polθ inhibitors, which substantially improved BEKI-mediated CAR KI efficiencies (**Fig. 3**). Consistent with previous reports[32], treatment with the DNA-PK inhibitor AZD7648 increased the frequency of kilobase deletions at the *TRAC* locus across editing platforms, including Cas9, Cas12a and BEKI. Importantly, co-treatment with the Polθ inhibitor ART558 reduced the frequency of these DNA-PK inhibitor induced kilobase-scale deletions. As described before[32], in the presence of a DNA repair template, we did not detect a significant increase of megabase-scale deletions. These findings confirm that while DNA-PK inhibition can increase the risk of large deletions, the concurrent presence of a repair template and inhibition of Polθ can

mitigate these effects, however further studies will be required to comprehensively assess long-term genomic stability and potential impacts on cellular fitness.

A concurrent study similarly demonstrated that base editors can be leveraged for double-nick–mediated transgene insertion, but relied on AAV-delivered donor templates[43]. Improved KI efficiency was achieved in a 'double-tap' approach, in which additional sgRNAs target base-editing byproducts to enable Iterative Nicking for Synchronous Engineered Reprogramming of T cells (INSERT)[43]. While AAV donor delivery may increase KI rates compared to dsDNA, viral templates introduce added complexity, cost, and regulatory burden[45,46]. Future improvements in KI rates could come from reducing donor toxicity, e.g. via transient DNA sensing inhibition[4], or by using modified single-stranded DNA (ssDNA) donor templates[48,49], which would allow higher template doses and promote HDR, although ssDNA may be prone to deamination by base editors[47].

CD3ζ-integrated CD19-CAR T cells generated with BEKI under transient DNA-PK and Polθ inhibition demonstrated in vivo antitumor activity in a xenograft Nalm6 lymphoma model (**Fig. 3C**). We then combined CAR KI with *RASA2* and *FKBP12* disruption, yielding triple-edited CAR T cells that displayed enhanced effector function under pharmacologic immunosuppression with tacrolimus or rapamycin. These findings illustrate the dual functionality of BEKI to mediate targeted KI and multiplex KO using a single enzyme (**Fig. 5A-B, Fig. S9**). Similar to approaches that confer resistance to lymphodepleting agents[25,48], engineering resistance to immunosuppressants could improve the persistence of allogeneic cells. We extended this strategy with additional *B2M* and *CIITA* edits for immune evasion. The resulting quintuple-edited allogeneic CAR T cells showed enhanced anti-tumor function and were protected from allo-specific rejection (**Fig. S11**). Finally, we used BEKI to generate *CD3ζ*-CAR T cells with

up to 10 additional KOs, illustrating that BEKI can sustain progressively complex editing strategies. While knock-in rates declined with increasing numbers of additional sgRNAs and requires further optimization, base editor-mediated knockout efficiencies remained stable. In the context of allogeneic CAR T cell therapies, eliminating residual $CD3^+$ cells is crucial to prevent GvHD and enables selective enrichment of CAR^+ cells, particularly as the CD3 KO efficiency using BEKI is lower than typically achieved with Cas9[49]. Notably, TCR/$CD3^-$ CAR^+ cells frequently harbored most of the additional knockouts, allowing enrichment of multi-edited cells through CD3 MACS depletion.

A key challenge in increasing the complexity of gene editing for cellular therapies is preserving genomic integrity while maintaining a feasible manufacturing process. In this study, we therefore performed an in-depth characterization of genomic alterations arising from different editing strategies, focusing on large deletions at on-target loci and chromosomal rearrangements following multiplex editing. When DNA repair pathways are pharmacologically modulated to enhance HDR, erroneous repair of induced DSBs can become more frequent. This was evident in our unbiased analysis of translocations following simultaneous targeting of *TRAC*, *RASA2* and *FKBP12* with a Cas9 nuclease. We detected both off-target cleavage events leading to off-target-mediated translocations and frequent rearrangements between the targeted loci themselves, with translocation frequencies further increased upon treatment with DNA-PK and Polθ inhibitors. Consistent with this increased genomic instability after conventional multiplex editing with Cas9 nuclease[50,51], we observed reduced cell viability during a 14-day expansion period (**Fig. S10**). By restricting DSB formation to the knock-in locus and performing additional edits through base editing, BEKI substantially reduced both on-target and off-target translocations, and we did not observe impaired cellular viability in these cells. These findings are consistent with

previous studies demonstrating that replacing multiplex Cas9 nuclease editing with base editing can improve engineered T cell products by increasing both editing efficiency and cellular fitness[50,52]. In addition, nuclease-induced DSBs have been reported to exert selective pressure that favors the survival of p53-deficient cells, whose reduced DNA damage sensitivity predisposes them to malignant transformation[53,54]. While our work focused on assessing and mitigating the risks associated with simultaneous DNA cleavage events, the use of base editors could result in off-target effects in the form of single nucleotide variants which are not detectable by the assays used in this study. The accompanying study describing the INSERT platform performed extensive off-target profiling using in silico predictions and RhAmpSeq for the specific sgRNAs used, and reported very low frequencies of unintended base editing. Because BEKI uses different sgRNAs, comprehensive off-target profiling will be required for each sgRNA in the final product prior to clinical application; the absence of such profiling here represents an important limitation of the present study.

Multiplex editing is attractive to engineer immune effector cells with enhanced therapeutic functionality; consequently, multiple manufacturing approaches have been explored that mitigate DSB-induced genotoxicity similar to BEKI and INSERT. Viral gene transfer combined with multiplex base editing reduces DSB-associated genotoxicity, but requires multiple editing steps and complicates manufacturing[29,50,55]. Transposases combined with base editing enable non-viral multiplexed editing in a single transfection[56]. However, random transgene integration by viral vectors and transposases has been associated with insertional mutagenesis and cases of secondary malignancies[57,58]. Gene editing methods that achieve high HDR rates, either by using AAV-delivered donor templates[59] or by selecting KI loci that inherently

allow enrichment of edited cells[60,61], minimize translocation risk by favoring the intended editing outcome. We and others have described multiplex editing platforms that combine CRISPR-Cas nuclease-mediated KI and multiple KOs in a single step, using orthogonal enzymes[41] or aptamer-extended sgRNAs[62] to direct DSBs and base edits to distinct loci. While these approaches enable precise multiplex editing with reduced translocation risks, the complexity of delivering multiple components limits clinical translation. New strategies such as peptide-mediated ribonucleoprotein (RNP) delivery (PERC)[63] and lipid nanoparticles (LNPs)[64] may improve feasibility by lowering the toxicities of electroporation and DNA template delivery, and by enabling temporal separation of editing steps. BEKI relies on paired nicking by D10A nCas9 creating a staggered DSB that stimulates HDR. This mechanism differs from DSB-independent integration platforms such as PASSIGE[65], PASTE[66] or CRISPR-associated transposases (CAST)[67]. Notably, integrase-based systems have demonstrated larger cargo capacity compared to conventional HDR-based approaches[68]. Potentially, BEKI could also be used to insert a landing-pad to guide large serine recombinases to specific sites[68].

The BEKI platform overcomes many of these challenges by enabling precise, non-viral KI and multiplex gene KOs in a single step with a single enzyme. By restricting DSBs to the KI site and employing base editing for gene KOs, this approach minimizes translocation risks and simplifies manufacturing by relying on a single editor, eliminating the need for orthogonal enzymes or viral components. Together, these features establish BEKI as a streamlined non-viral platform for the safe and efficient multiplex engineering in a single intervention, exemplified by the generation of quintuple-edited allogeneic CAR T cells, representing a step towards more effective and accessible T cell therapies.

Materials and Methods

PBMC isolation and T cell enrichment

Peripheral blood was collected from healthy adult donors with informed consent under Charité ethics approval (EA4/091/19 and EA1/052/22), in accordance with the Declaration of Helsinki. Blood drawn into 10 mL lithium-heparin tubes (BD) was diluted 1:1 with sterile PBS (Gibco) and layered onto 15 mL of Pancoll (PAN Biotech) or Biocoll (Bio&SELL) in Leucosep™ tubes (Greiner). Samples were centrifuged at 800 × g for 20 minutes at room temperature without brake. The PBMC layer was collected from the interface, washed twice with PBS (300 × g, 10 min), and viable cells were counted using a Neubauer chamber and trypan blue exclusion (Sigma-Aldrich).

Prior to T cell seeding, 24-well tissue culture plates were coated with 1 µg/mL each of anti-CD3 (Invitrogen) and anti-CD28 (BioLegend) in 0.5 mL/well sterile water (Ampuwa), sealed with parafilm, and incubated at 4 °C for 24 h. Human $CD3^+$ T cells were enriched from PBMCs via magnetic cell separation (MACS, Miltenyi Biotec) following the manufacturer's protocol. In brief, cells were resuspended in cold MACS buffer (PBS + 2% heat-inactivated FCS + 2 mM EDTA), incubated with anti-CD3-conjugated magnetic beads for 15 min at 4 °C, washed, filtered (30 µm), and separated using LS columns (Miltenyi Biotec). Isolated cells were counted and seeded at 0.75 × 10^6 cells/mL into pre-washed αCD3/αCD28-coated wells.

Cell culture

T cells were cultured at 37 °C and 5% CO_2 in CTL medium consisting of 1:1 Advanced RPMI and Click's Medium with 1% GlutaMAX supplemented with 10% heat-inactivated FCS (Biochrom or Sigma-Aldrich), 10 ng/mL IL-7, and 5 ng/mL IL-15 (CellGenix). Antibiotics were omitted due to their negative impact on post-electroporation viability.

Nalm-6 cells were cultured in RPMI 1640 with 10% FCS, 100 IU/mL penicillin, and 100 µg/mL streptomycin, and passaged every 2–3 days. For the animal experiment, the T cells were seeded in G-Rex bioreactors (ScaleReady) for expansion post-electroporation.

Plasmid construction and cloning

Cloning strategies were planned with SnapGene. Multiple-fragment In-Fusion cloning (Takara Bio) was performed using purified PCR fragments (KAPA HiFi HotStart, Roche) designed with primers generating 15 bp overlaps. In-Fusion reactions (5 µL) were transformed into 10 µL Stellar Competent *E. coli*, plated on LB-ampicillin agar, and incubated at 37 °C overnight. Colonies were screened by PCR using M13 universal primers flanking the pUC19 insertion site. Positive clones were grown in 5 mL LB/ampicillin overnight, and plasmids were purified (ZymoPURE Mini Prep Kit, Zymo Research). Sequence integrity of plasmids was confirmed via Sanger sequencing (LGC Genomics, Eurofins).

In vitro transcription (IVT) of mRNA

ABE8.20-m (Addgene #136300) and BE4_RrA3F (Addgene #138340) from Gaudelli *et al*.[39,69] were cloned into plasmids containing a dT7 promoter, Kozak sequence, and 5′/3′ UTRs (TriLink). In addition, a D10A nickase Cas9 was derived from ABE8.20-m using In-Fusion cloning (Takara), and a wild-type Cas9 construct was generated by correcting the D10A mutation. Linear PCR templates were generated using KAPA HiFi HotStart (Roche), installing the correct T7 promoter sequence and a 120 bp polyA tail. PCR products were purified (Zymo DNA Clean & Concentrator-5) and IVT was performed using the HiScribe™ T7 High Yield RNA Synthesis Kit (NEB) with N1-methyl-pseudouridine (TriLink) and CleanCap AG (TriLink) for co-transcriptional

capping. Template DNA was removed with DNase I (NEB), and mRNA was purified using the Monarch® RNA Cleanup Kit (NEB). RNA integrity was assessed via 1.5% denaturing agarose gel electrophoresis using RNA loading dye and ssRNA ladder (NEB). Finally, the mRNA concentration was measured using a Qubit fluorometer with the RNA BR Assay (Thermo Fisher Scientific), diluted to 2 µg/µL and stored at −80 °C.

Generation and modification of dsDNA HDRTs for CAR insertion

HDR donor templates (HDRTs) were engineered for targeted insertion of a second-generation CD19 chimeric antigen receptor (CAR) into the *TRAC* locus, a truncated CAR lacking CD3ζ into the *CD3ζ* locus, an HLA-E–B2M fusion construct into *B2M* and a TCR fusion construct (TRuC) into *CD3ε*. Previously described HDRTs (*TRAC*[2], *CD3ζ*[3], *B2M*[11], *CD3ε*[38]) were modified for improved compatibility with nickase-based editing by adjusting homology arms (HAs) to flank the generated DNA nicks (**Table S1**). In some cases, HAs were adapted to accommodate multiple proximal sgRNAs by positioning HA ends within 35 bp of the nick site. Where HDRTs included sequences homologous to the sgRNA, silent PAM mutations were introduced to prevent re-cleavage. Multiple-fragment In-Fusion cloning (Clontech, Takara) was used to assemble HDRTs from overlapping PCR products generated with KAPA HiFi HotStart 2x Readymix (Roche). For HDRT generation, 500 µL PCR reactions were performed and purified using AMPure XP paramagnetic beads (Beckman Coulter) with two 70% ethanol washes. Purified HDRTs were quantified using a Nanodrop spectrophotometer (Thermo Fisher Scientific) and adjusted to a concentration of 1 or 2 µg/µL in nuclease-free water.

Gene Editing

Primary human T cells were harvested ~48 hours after anti-CD3/CD28 stimulation, counted, and washed twice in sterile PBS by centrifugation at 100 × g for 10 min at room temperature (RT).

mRNA-based knock-in

Double nick-mediated knock-ins were performed by co-electroporating: (1) HDR donor template (1 µL, 1–2 µg/µL), (2) two strand-specific sgRNAs (0.48 µL each, 100 µM; IDT), and (3) mRNA encoding the base or nuclease editor (1 µL, 2 µg/µL). Optionally, additional sgRNAs for base editing were included. Reagents were assembled in PCR strips by adding components sequentially. Synthetic, chemically modified sgRNAs (or crRNAs for Cas12a; IDT) were resuspended in nuclease-free 1×TE buffer and stored at −20 °C (**Table S2**). sgRNAs for splice site disruption using base editors were designed using SpliceR[30]. Previously published sgRNAs targeting *TRAC*, *B2M*[39], *CIITA*[39], *CD54, CD58, CD38, CD2*[70], *CD5*[71] and *CD7*[71] were used.

Cas12a Ribonucleoprotein (RNP)-based knock-in

For Cas12a RNP assembly, 0.5 µL of 100 µg/µL poly(L-glutamic acid) (PGA; 15–50 kDa; Sigma-Aldrich) was combined with 0.48 µL *TRAC*-specific CRISPR-RNA (crRNA) (IDT) and mixed thoroughly. Then, 0.4 µL of Alt-R A.s. Cas12a Ultra (IDT; 10 µg/µL) was added and incubated for 15 min at RT to form RNPs, followed by addition of 1 µL HDRT (1-2 µg/µL). The mixture was kept on ice until electroporation.

Electroporation

Cells were resuspended in 20 µL of ice-cold P3 electroporation buffer (Lonza) at a concentration of 1–1.5 × 10^6 cells per reaction and immediately used for electroporation. The cell suspensions were mixed with the prepared reagent mix and transferred to a 16-well electroporation strip (Lonza). To ensure proper contact and

eliminate air bubbles, strips were gently tapped on the bench before electroporation. Electroporation was performed on a 4D-Nucleofector (Lonza) using program EH-115. Immediately after, 100 µL of pre-warmed T cell medium was added per well and the cells were placed in the incubator for 10 min. Cells were then gently resuspended and equally divided into two separate wells of a 96-well round-bottom plate, each containing 150 µL of pre-warmed T cell medium, resulting in a final density of 0.5–0.75 × 10^6 cells per well. For the animal experiment, three electroporation reactions were performed and subsequently seeded together in one well of a G-Rex®24 Well Plate (3M cells per well).

HDR enhancing drugs:

For pharmacological HDR enhancement, the 150 µL culture medium was supplemented with a DNA-PK inhibitor, either HDR Enhancer v2 (0.5 µM, IDT), nedisertib (M3814, 2 µM, Selleckchem), or AZD7648 (0.5 µM, MedChemExpress), with the optional addition of a Polθ inhibitor, either novobiocin (10 µM, MedChemExpress) or ART558 (1 µM, GLPBIO), unless stated otherwise. A medium change or initial cell split was performed within 24 hours post-electroporation using HDR enhancer-free T cell medium. Cells were subsequently expanded in 96-well round-bottom or 24-well plates and split every 2-3 days.

Flow Cytometry

Flow cytometry was used to assess gene editing efficiency on day 4 post-electroporation and to evaluate the functionality of the generated CAR T cells. All measurements were performed on a CytoFLEX LX (Beckman Coulter) and analyzed using FlowJo v10 (BD).

Cells were transferred to 96-well U-bottom plates and washed with PBS (centrifuged at 400 g for 5 min at room temperature). A staining master mix containing fluorophore-

615 conjugated antibodies was prepared in PBS and added at 20 µL per well. Cells were
616 incubated for 15 min at 4 °C unless otherwise specified, followed by one or two PBS
617 washes prior to acquisition. To prevent cross-reactivity from the anti-Fc antibody used
618 for CAR detection, extracellular staining began with anti-Fc AF647 and a viability dye,
619 followed by two washes before staining additional surface markers.
620
621 **Animal experiment**
622 Experiments involving mice were performed at Baylor College of Medicine in
623 compliance and with approval from the Institutional Animal Care and Use Committee
624 (IACUC) under ID: AN-5551. In brief, immunodeficient mice were infused with 0.5 ×
625 10^6 Nalm-6 cells (expressing GFP and firefly luciferase) via tail vein injection. Seven
626 days later, 0.5 × 10^6 CAR^+ T cells were infused intravenously. *TRAC* KO T cells were
627 injected at the same total number as the TCR-deficient *CD3ζ*-CAR T cells. T cells were
628 cryo-preserved in FCS supplemented with 10% DMSO on day 14 post blood collection
629 then thawed, washed and formulated in PBS 3 hours prior to application. Tumor burden
630 was assessed using bioluminescence imaging. Mice were anesthetized with Isoflurane
631 and received intraperitoneally 150 mg/kg D-Luciferin (Revvity) dissolved in water. BLI
632 was performed with the In Vivo Imaging System (Lumina III, Revvity). Animal welfare,
633 body weights and general health conditions were controlled. Mice were euthanized
634 after individual evaluation for each mouse with body weight loss >20% or ethical end
635 points reached.
636
637 **Cytotoxicity Assay of Allo-Reactive T Cells Against Multiplexed Gene-Edited T**
638 **Cells**
639 To assess resistance of gene-edited T cells to allo-reactive killing, allo-reactive T cells
640 were preferentially expanded using HLA mismatched allogeneic feeder cells for

allogeneic stimulation. $CD8^+$ T cells were enriched by MACS and co-cultured 1:1 with irradiated (30 Grey), CD3-depleted PBMCs from a second donor on the day of isolation and again on day 7, followed by expansion. 1 day after stimulation with feeder cells, T cell medium containing cytokines (10 ng/mL IL-7 and 5 ng/mL IL-15) was added for cell expansion.

Cytotoxicity assays were performed using target T cells (mock-electroporated or gene-edited lacking HLA class I and II expression) from the same donor used for allogeneic stimulation. 25,000 CFSE (Thermo Fisher Scientific) labeled target cells were seeded per well in 96-well round-bottom plates. Allo-reactive effector T cells were added at varying effector-to-target (E:T) ratios (2:1 to 0.5:1) and wells containing only target cells served as controls. Plates were briefly centrifuged (100 g, 1 min, RT) and incubated for 16 h at 37 °C and 5% CO_2. For the readout, 100 µL of cell suspension was mixed with 100 µL of DAPI in PBS (1:10,000), incubated at 4 °C for ≥10 min, and 30 µL were acquired on a flow cytometer. Cytotoxicity was quantified based on the number of viable $CFSE^+$ target cells compared to target-only controls.

Nalm6 co-culture assay

For intracellular cytokine assessment 100,000 effector cells were co-cultured with target cells at a 1:1 ratio in 96-well round-bottom plates for 6 hours without or with tacrolimus at a final concentration of 6 ng/mL. After 1 hour, brefeldin A (Sigma Aldrich, Cat# B5936) was added to the suspension to reach a final concentration of 10 µg/ml. After another 5 hours of co-culture the intracellular staining was performed using the Intracellular Fixation & Permeabilization Buffer Set (Thermo Fisher).

CAR-T cells tumor control was assessed in vitro via live cell imaging of GFP-expressing Nalm6 tumor cells on an Incucyte device (Sartorius) in phenol red-free RPMI 1640 media (Gibco). CAR-T cells were expanded for 14 days following

electroporation and subsequently rested for 24 hours in cytokine-free medium prior to the assay. A total of 2 x 10^4 GFP-labeled Nalm-6 cells were seeded into a flat-bottom 96-well plates and co-cultured in a 10:1 target-to-effector cell ratio with T cells without or with 100 nM rapamycin. To account for differences in initial editing efficiencies, all effector samples were adjusted to the same frequency of CAR^+ T cells with *TRAC*-KO cells, ensuring an equal total cell number across conditions. The plates were then placed into the Incucyte device and a repeat scanning was performed over 48 hours with scans taken every 2 hours, capturing three images per well.

Sanger Sequencing and Gene Editing Quantification

To quantify gene editing efficiency at the DNA level, genomic DNA (gDNA) was isolated on day 14 post-electroporation using the DNeasy Blood and Tissue Kit (Qiagen). Target regions at the *RASA2* and *FKBP12* loci were amplified via PCR using KAPA HiFi polymerase (Roche) with primers designed in COSMID[72] to generate 500–700 bp amplicons. Primer specificity was confirmed in silico using Primer-BLAST[73] and validated by electrophoresis on a 1.5% agarose gel. PCR products were purified using the DNA Clean & Concentrator-5 Kit (Zymo Research) and submitted for Sanger sequencing (LGC Genomics). The used primers are listed in **Table S3**.

Base editing efficiency was quantified using EditR[74] and indel frequencies were estimated using ICE analysis[75] (Synthego). Genomic DNA from mock-electroporated cells of the same donors served as negative controls for both analyses.

On-target long-read Nanopore sequencing

500 ng of genomic DNA was amplified using NEBNext Ultra II Q5 HiFi polymerase (New England Biolabs) with primers containing stubbers for downstream indexing. The following PCR cycle conditions were used: denaturation at 98 °C for 30s followed by

25 cycles of 98 °C for 10 s, 60 °C for 30 s, and 72 °C for 10 min. PCR products were purified with 0.8X SPRI beads and eluted in H2O. Sequencing-compatible libraries were generated using the PCR Barcoding Expansion 1-96 [EXP-PBC096] for Ligation Sequencing Kit [SQK-LSK114] (Oxford Nanopore). A second round of PCR was performed using identical cycling conditions for six cycles to index the amplicons. Purified libraries were quantified by Qubit High-Sensitivity DNA assay and sequenced on a PromethION 24 with the R10.4.1 flow cell (Oxford Nanopore).

Reads lengths were quantified using SummarizeOntDels (https://github.com/cornlab/summarizeOntDeletions)[32] by aligning to a pseudo-genome containing the expected HR allele.

CAST-Seq

Genomic DNA was extracted using the NucleoSpin Tissue kit (Macherey-Nagel). CAST-Seq analyses were performed following the previously described protocol[76], with some adjustments to the workflow[77]. In brief, the average fragmentation size of the genomic DNA was aimed at a length of 500 bp. The libraries were sequenced on a NovaSeq 6000 using 2 × 150 bp paired-end sequencing (GENEWIZ, Azenta Life Sciences). Changes were made to the bioinformatic pipeline to enhance specificity. Sites under investigation were categorized as OMT if the p value met the cutoff of 0.005. In addition, further features were incorporated in the CAST-Seq algorithm, including barcode hopping annotation and an update to the coverage analysis to reduce the execution time by aligning the gRNAs only to the most covered regions for each site. Two technical replicates from samples of two different donors were used for the CAST-Seq analysis. Only sites identified as significant in at least 3 out of the total 4 replicates were considered as putative events.

Digital droplet polymerase chain reaction (ddPCR)

To quantify chromosomal translocations, ddPCR assays were designed to detect balanced translocations involving the *TRAC, RASA2*, or *FKBP12* loci (**Table S3**). The RPP30 gene served as a reference control, as previously described.

For each reaction, 75 ng of genomic DNA digested with HindIII-HF (NEB, Germany) was used as the template in a 22 µL ddPCR mix containing:

- 5.5 µL of 4x dPCR Multiplex Supermix (Bio-Rad)
- 1.25 µL (10 µM) of each forward and reverse primer for the reference gene
- 1.25 µL (5 µM) of FAM-labeled probe for the reference gene
- 1.25 µL (10 µM) of each forward and reverse primer for the target gene
- 1.25 µL (5 µM) of HEX-labeled probe for the target gene
- Nuclease-free water

Droplet generation was carried out using the QX200 Droplet Generator (Bio-Rad) by loading 20 µL of sample mix and 70 µL of droplet generation oil into a DG8™ Cartridge, sealed with a DG8™ Gasket. Empty wells were filled with ddPCR Buffer Control.

Following droplet generation, droplets were carefully transferred into a 96-well PCR plate, sealed with pierceable foil using the PX1™ PCR Plate Sealer at 185 °C for 5 s. PCR was performed according to the manufacturer's cycling protocol. Samples generating fewer than 15,000 accepted droplets or more than 99% positive droplets for the reference gene (*RPP30*) were excluded and repeated.

For the ddPCR for Mb scale-deletions a target probe was designed that binds within the *ZHFX2* gene, 1 Mb downstream (towards the telomere) of the *TRAC* gene and a control probe within *KM2TC* on a different chromosome. The ddPCR was performed as described above except for using 250 ng of DNA per 22 µl reaction and the following cycling conditions: 10 min at 95 °C, then 40 cycles of 30 s at 94 °C and 1 min at 57 °C, followed by 10 min at 98 °C.

745

746 **Data Analysis, visualization and text editing**

747 Experimental data were collected in Excel and analyzed using GraphPad Prism 9, with
748 statistical methods detailed in the main text. Figures and schematics were created in
749 BioRender.com. Text clarity and grammar were improved using ChatGPT (OpenAI).

750

Availability of data and materials

The ABE8.20m and BE4 were gifts from Nicole Gaudelli (Addgene plasmid #136300 and #138340). The original HDR templates for *TRAC* and *CD3ζ* were deposited with Addgene (Addgene plasmids #215769 and #215759). To encourage broad adoption of BEKI, the BEKI-adapted HDR template plasmids for CD19-CAR knock-in at *TRAC* and *CD3ζ* (*CD247*) have also been deposited with Addgene (Addgene plasmids #247056 and #247057). The IVT plasmid backbone contains proprietary 5'-UTR and 3'-UTR sequences and was procured from TriLink Inc. under a non-disclosure agreement. All other construct sequences can be found in **Table S1.**

Acknowledgements

The authors would like to thank Cliona Rooney and Lisa Rollins (both, Baylor College of Medicine) for their help in the animal studies.

Ethics approval and consent to participate: The study was performed in accordance with the Declaration of Helsinki. Peripheral blood from healthy human donors was obtained after informed and written consent (Charité ethics committee approval EA4/091/19 and EA1/052/22, Baylor College of Medicine IRB approval H-45017).

Funding: The project received funding from the European Union under grant agreement no. 101057438 (geneTIGA: genetiga-horizon.eu) to T.Ca., H.-D.V., P.R. and D.L.W. Views and opinions expressed are those of the author(s) only and do not necessarily reflect those of the European Union or the European Health and Digital Executive Agency (HADEA). Neither the European Union nor the granting authority can be held responsible for them. V.G., J.K. and D.L.W. were supported by the SPARK-BIH Program by the Berlin Institute of Health, Germany. The study received support for reagents provided by ScaleReady through the G-Rex Grant Initiative (M.P., D.L.W. – Baylor College of Medicine). Parts of the study were supported by the

National Cancer Institute of the National Institutes of Health (SPORE in Lymphoma, Grant Lymphoma SPORE, Grant 5 P50 CA126752-20) and the Cancer Research & Prevention Institute of Texas (CPRIT RP240545).

We also acknowledge funding from the German Federal Ministry of Education and Research (BMBF) within the Medical Informatics Funding Scheme EkoEstMed–FKZ 01ZZ2015 (G.A.).

Author contributions

VG designed the study, planned and performed experiments, analyzed results, interpreted the data, and wrote the manuscript. L.J.B., C.F.-G., E.J.A. L.H., L.M.H, A.-M.N., Y.P., C.L.F., I.K. and M.P. performed experiments, analyzed results, interpreted data and edited the manuscript. M.S., R.K. and S.S. performed experiments, analyzed results and interpreted data. G.A. analyzed and interpreted CAST-seq data. J.E.C. supervised long read sequencing and ddPCR analysis, provided reagents, interpreted data, and edited the manuscript. T.Ca. supervised CAST-Seq analysis, provided reagents, interpreted data, and edited the manuscript. H.-D.V. and P.R. provided reagents, interpreted data, and edited the manuscript. J.K. and D.L.W. designed and led the study, planned experiments, interpreted data, and wrote the manuscript. All authors discussed, commented on, and approved the manuscript in its final form.

Declaration of Interests

V.G., J.K., D.L.W., H.-D.V., P.R. are named as inventors on patent applications filed by Charité – Universitätsmedizin Berlin, describing parts of this work (EP24222163.8 – BEKI system, D.L.W., V.G., J.K.; CD3-zeta editing: EP4019538A1 – D.L.W., J.K., H.-D.V., P.R.; CD3-epsilon editing: EP4353252A1 – D.L.W., J.K., H.-D.V., P.R.). T.Ca. and G.A. are co-inventors of CAST-Seq (patent US11319580B2). The Wagner Lab at

Charité has received reagents related to gene editing from IDT and GenScript Inc. P.R., H.-D.V. and D.L.W. are co-founders of the startup TCBalance Biopharmaceuticals GmbH focused on regulatory T cell therapy, which was not involved in the present study. H.-D.V. is founder and CSO at CheckImmune GmbH. D.L.W.'s laboratory at Baylor College of Medicine received reagents from ScaleReady through the G-Rex Grant initiative. J.E.C. is a co-founder and SAB member of Serac Biosciences and an SAB member of Relation Therapeutics, Hornet Bio, and Kano Therapeutics. The lab of J.E.C. has had funded collaborations with Allogene, Cimeio, and Serac. None of these companies were involved in the present study. All other authors declare that they do not have competing interests.

814 ## Keywords

815 CRISPR, Cas9, base editing, Cas12a, translocations, gene editing, non-viral gene
816 transfer, chimeric antigen receptors, CAR T cells, off-the-shelf

References

1. Mueller, K.P., Piscopo, N.J., Forsberg, M.H., Saraspe, L.A., Das, A., Russell, B., Smerchansky, M., Cappabianca, D., Shi, L., Shankar, K., et al. (2022). Production and characterization of virus-free, CRISPR-CAR T cells capable of inducing solid tumor regression. J Immunother Cancer *10*, e004446. https://doi.org/10.1136/jitc-2021-004446.

2. Roth, T.L., Puig-Saus, C., Yu, R., Shifrut, E., Carnevale, J., Li, P.J., Hiatt, J., Saco, J., Krystofinski, P., Li, H., et al. (2018). Reprogramming human T cell function and specificity with non-viral genome targeting. Nature *559*, 405–409. https://doi.org/10.1038/s41586-018-0326-5.

3. Kath, J., Franke, C., Drosdek, V., Du, W., Glaser, V., Fuster-Garcia, C., Stein, M., Zittel, T., Schulenberg, S., Porter, C.E., et al. (2024). Integration of ζ-deficient CARs into the CD3ζ gene conveys potent cytotoxicity in T and NK cells. Blood *143*, 2599–2611. https://doi.org/10.1182/blood.2023020973.

4. Kath, J., Du, W., Pruene, A., Braun, T., Thommandru, B., Turk, R., Sturgeon, M.L., Kurgan, G.L., Amini, L., Stein, M., et al. (2022). Pharmacological interventions enhance virus-free generation of TRAC-replaced CAR T cells. Mol Ther Methods Clin Dev *25*, 311–330. https://doi.org/10.1016/j.omtm.2022.03.018.

5. Eyquem, J., Mansilla-Soto, J., Giavridis, T., van der Stegen, S.J.C., Hamieh, M., Cunanan, K.M., Odak, A., Gönen, M., and Sadelain, M. (2017). Targeting a CAR to the TRAC locus with CRISPR/Cas9 enhances tumour rejection. Nature *543*, 113–117. https://doi.org/10.1038/nature21405.

6. Qasim, W., Zhan, H., Samarasinghe, S., Adams, S., Amrolia, P., Stafford, S., Butler, K., Rivat, C., Wright, G., Somana, K., et al. (2017). Molecular remission of infant B-ALL after infusion of universal TALEN gene-edited CAR T cells. Sci Transl Med *9*. https://doi.org/10.1126/scitranslmed.aaj2013.

7. Torikai, H., Reik, A., Liu, P.-Q., Zhou, Y., Zhang, L., Maiti, S., Huls, H., Miller, J.C., Kebriaei, P., Rabinovich, B., et al. (2012). A foundation for universal T-cell based immunotherapy: T cells engineered to express a CD19-specific chimeric-antigen-receptor and eliminate expression of endogenous TCR. Blood *119*, 5697–5705. https://doi.org/10.1182/blood-2012-01-405365.

8. Wagner, D.L., Koehl, U., Chmielewski, M., Scheid, C., and Stripecke, R. (2022). Review: Sustainable Clinical Development of CAR-T Cells - Switching From Viral Transduction Towards CRISPR-Cas Gene Editing. Front Immunol *13*, 865424. https://doi.org/10.3389/fimmu.2022.865424.

9. Wang, D., Quan, Y., Yan, Q., Morales, J.E., and Wetsel, R.A. (2015). Targeted Disruption of the *β* 2-Microglobulin Gene Minimizes the Immunogenicity of Human Embryonic Stem Cells. Stem Cells Translational Medicine *4*, 1234–1245. https://doi.org/10.5966/sctm.2015-0049.

10. Scharer, C.D., Choi, N.M., Barwick, B.G., Majumder, P., Lohsen, S., and Boss, J.M. (2015). Genome-wide CIITA-binding profile identifies sequence preferences that dictate function versus recruitment. Nucleic Acids Research *43*, 3128–3142. https://doi.org/10.1093/nar/gkv182.

11. McCallion, O., Du, W., Glaser, V., Milward, K., Franke, C., Kath, J., Valkov, M., Yang, M., Künkele, A., Polansky, J.K., et al. (2023). Matching or genetic engineering of HLA Class I and II facilitates successful allogeneic 'off-the-shelf' regulatory T cell therapy. Preprint at bioRxiv, https://doi.org/10.1101/2023.08.06.551956 https://doi.org/10.1101/2023.08.06.551956.

12. Cherkassky, L., Morello, A., Villena-Vargas, J., Feng, Y., Dimitrov, D.S., Jones, D.R., Sadelain, M., and Adusumilli, P.S. (2020). Human CAR T cells with cell-intrinsic PD-1 checkpoint blockade resist tumor-mediated inhibition. J Clin Invest *126*, 3130–3144. https://doi.org/10.1172/JCI83092.

13. Tang, N., Cheng, C., Zhang, X., Qiao, M., Li, N., Mu, W., Wei, X.-F., Han, W., and Wang, H. (2020). TGF-β inhibition via CRISPR promotes the long-term efficacy of CAR T cells against solid tumors. JCI Insight *5*, e133977. https://doi.org/10.1172/jci.insight.133977.

14. Amini, L., Wagner, D.L., Rössler, U., Zarrinrad, G., Wagner, L.F., Vollmer, T., Wendering, D.J., Kornak, U., Volk, H.-D., Reinke, P., et al. (2020). CRISPR-Cas9-Edited Tacrolimus-Resistant Antiviral T Cells for Advanced Adoptive Immunotherapy in Transplant Recipients. Molecular Therapy *0*. https://doi.org/10.1016/j.ymthe.2020.09.011.

15. Wei, J., Long, L., Zheng, W., Dhungana, Y., Lim, S.A., Guy, C., Wang, Y., Wang, Y.-D., Qian, C., Xu, B., et al. (2019). Targeting REGNASE-1 programs long-lived effector T cells for cancer therapy. Nature *576*, 471–476. https://doi.org/10.1038/s41586-019-1821-z.

16. Adachi, Y., Terakura, S., Osaki, M., Okuno, Y., Sato, Y., Sagou, K., Takeuchi, Y., Yokota, H., Imai, K., Steinberger, P., et al. (2024). Cullin-5 deficiency promotes chimeric antigen receptor T cell effector functions potentially via the modulation of JAK/STAT signaling pathway. Nat Commun *15*, 10376. https://doi.org/10.1038/s41467-024-54794-x.

17. Cheng, J., Xiao, Y., Peng, T., Zhang, Z., Qin, Y., Wang, Y., Shi, J., Yan, J., Zhao, Z., Zheng, L., et al. (2025). ETV7 limits the antiviral and antitumor efficacy of CD8+ T cells by diverting their fate toward exhaustion. Nat Cancer *6*, 338–356. https://doi.org/10.1038/s43018-024-00892-0.

18. Trefny, M.P., Kirchhammer, N., Auf Der Maur, P., Natoli, M., Schmid, D., Germann, M., Fernandez Rodriguez, L., Herzig, P., Lötscher, J., Akrami, M., et al. (2023). Deletion of SNX9 alleviates CD8 T cell exhaustion for effective cellular cancer immunotherapy. Nat Commun *14*, 86. https://doi.org/10.1038/s41467-022-35583-w.

19. Freitas, K.A., Belk, J.A., Sotillo, E., Quinn, P.J., Ramello, M.C., Malipatlolla, M., Daniel, B., Sandor, K., Klysz, D., Bjelajac, J., et al. (2022). Enhanced T cell effector activity by targeting the Mediator kinase module. Science *378*, eabn5647. https://doi.org/10.1126/science.abn5647.

20. Shifrut, E., Carnevale, J., Tobin, V., Roth, T.L., Woo, J.M., Bui, C.T., Li, P.J., Diolaiti, M.E., Ashworth, A., and Marson, A. (2018). Genome-wide CRISPR Screens in Primary Human T Cells Reveal Key Regulators of Immune Function. Cell *175*, 1958-1971.e15. https://doi.org/10.1016/j.cell.2018.10.024.

21. Carnevale, J., Shifrut, E., Kale, N., Nyberg, W.A., Blaeschke, F., Chen, Y.Y., Li, Z., Bapat, S.P., Diolaiti, M.E., O'Leary, P., et al. (2022). RASA2 ablation in T cells boosts antigen sensitivity and long-term function. Nature *609*, 174–182. https://doi.org/10.1038/s41586-022-05126-w.

22. Alanis-Lobato, G., Zohren, J., McCarthy, A., Fogarty, N.M.E., Kubikova, N., Hardman, E., Greco, M., Wells, D., Turner, J.M.A., and Niakan, K.K. (2021). Frequent loss of heterozygosity in CRISPR-Cas9–edited early human embryos. Proc. Natl. Acad. Sci. U.S.A. *118*, e2004832117. https://doi.org/10.1073/pnas.2004832117.

23. Lazar, N.H., Celik, S., Chen, L., Fay, M.M., Irish, J.C., Jensen, J., Tillinghast, C.A., Urbanik, J., Bone, W.P., Gibson, C.C., et al. (2024). High-resolution genome-wide mapping of chromosome-arm-scale truncations induced by CRISPR–Cas9 editing. Nat Genet *56*, 1482–1493. https://doi.org/10.1038/s41588-024-01758-y.

24. Nahmad, A.D., Reuveni, E., Goldschmidt, E., Tenne, T., Liberman, M., Horovitz-Fried, M., Khosravi, R., Kobo, H., Reinstein, E., Madi, A., et al. (2022). Frequent aneuploidy in primary human T cells after CRISPR–Cas9 cleavage. Nat Biotechnol, 1–7. https://doi.org/10.1038/s41587-022-01377-0.

25. Qasim, W., Zhan, H., Samarasinghe, S., Adams, S., Amrolia, P., Stafford, S., Butler, K., Rivat, C., Wright, G., Somana, K., et al. (2017). Molecular remission of infant B-ALL after infusion of universal TALEN gene-edited CAR T cells. Sci Transl Med *9*. https://doi.org/10.1126/scitranslmed.aaj2013.

26. Mitelman, F., Johansson, B., and Mertens, F. (2007). The impact of translocations and gene fusions on cancer causation. Nat Rev Cancer *7*, 233–245. https://doi.org/10.1038/nrc2091.

27. Komor, A.C., Kim, Y.B., Packer, M.S., Zuris, J.A., and Liu, D.R. (2016). Programmable editing of a target base in genomic DNA without double-stranded DNA cleavage. Nature *533*, 420–424. https://doi.org/10.1038/nature17946.

28. Gaudelli, N.M., Komor, A.C., Rees, H.A., Packer, M.S., Badran, A.H., Bryson, D.I., and Liu, D.R. (2017). Programmable base editing of A•T to G•C in genomic DNA without DNA cleavage. Nature *551*, 464–471. https://doi.org/10.1038/nature24644.

29. Webber, B.R., Lonetree, C., Kluesner, M.G., Johnson, M.J., Pomeroy, E.J., Diers, M.D., Lahr, W.S., Draper, G.M., Slipek, N.J., Smeester, B.A., et al. (2019). Highly efficient multiplex human T cell engineering without double-strand breaks using

Cas9 base editors. Nat Commun *10*, 5222. https://doi.org/10.1038/s41467-019-13007-6.

30. Kluesner, M.G., Lahr, W.S., Lonetree, C., Smeester, B.A., Qiu, X., Slipek, N.J., Claudio Vázquez, P.N., Pitzen, S.P., Pomeroy, E.J., Vignes, M.J., et al. (2021). CRISPR-Cas9 cytidine and adenosine base editing of splice-sites mediates highly-efficient disruption of proteins in primary and immortalized cells. Nat Commun *12*, 2437. https://doi.org/10.1038/s41467-021-22009-2.

31. Kuscu, C., Parlak, M., Tufan, T., Yang, J., Szlachta, K., Wei, X., Mammadov, R., and Adli, M. (2017). CRISPR-STOP: gene silencing through base-editing-induced nonsense mutations. Nat Methods *14*, 710–712. https://doi.org/10.1038/nmeth.4327.

32. Cullot, G., Aird, E.J., Schlapansky, M.F., Yeh, C.D., Van De Venn, L., Vykhlyantseva, I., Kreutzer, S., Mailänder, D., Lewków, B., Klermund, J., et al. (2024). Genome editing with the HDR-enhancing DNA-PKcs inhibitor AZD7648 causes large-scale genomic alterations. Nat Biotechnol. https://doi.org/10.1038/s41587-024-02488-6.

33. Wimberger, S., Akrap, N., Firth, M., Brengdahl, J., Engberg, S., Schwinn, M.K., Slater, M.R., Lundin, A., Hsieh, P.-P., Li, S., et al. (2023). Simultaneous inhibition of DNA-PK and Polϴ improves integration efficiency and precision of genome editing. Nat Commun *14*, 4761. https://doi.org/10.1038/s41467-023-40344-4.

34. Ran, F.A., Hsu, P.D., Lin, C.-Y., Gootenberg, J.S., Konermann, S., Trevino, A.E., Scott, D.A., Inoue, A., Matoba, S., Zhang, Y., et al. (2013). Double nicking by RNA-guided CRISPR Cas9 for enhanced genome editing specificity. Cell *154*, 1380–1389. https://doi.org/10.1016/j.cell.2013.08.021.

35. Mali, P., Aach, J., Stranges, P.B., Esvelt, K.M., Moosburner, M., Kosuri, S., Yang, L., and Church, G.M. (2013). CAS9 transcriptional activators for target specificity screening and paired nickases for cooperative genome engineering. Nat Biotechnol *31*, 833–838. https://doi.org/10.1038/nbt.2675.

36. Tran, N.T., Danner, E., Li, X., Graf, R., Lebedin, M., de la Rosa, K., Kühn, R., Rajewsky, K., and Chu, V.T. (2022). Precise CRISPR-Cas-mediated gene repair with minimal off-target and unintended on-target mutations in human hematopoietic stem cells. Sci Adv *8*, eabm9106. https://doi.org/10.1126/sciadv.abm9106.

37. Jinek, M., Chylinski, K., Fonfara, I., Hauer, M., Doudna, J.A., and Charpentier, E. (2012). A programmable dual-RNA-guided DNA endonuclease in adaptive bacterial immunity. Science *337*, 816–821. https://doi.org/10.1126/science.1225829.

38. Du, W., Noyan, F., McCallion, O., Drosdek, V., Kath, J., Glaser, V., Fuster-Garcia, C., Yang, M., Stein, M., Franke, C., et al. (2025). Gene editing of CD3 epsilon to redirect regulatory T cells for adoptive T cell transfer. Mol Ther *33*, 997–1013. https://doi.org/10.1016/j.ymthe.2025.01.045.

39. Gaudelli, N.M., Lam, D.K., Rees, H.A., Solá-Esteves, N.M., Barrera, L.A., Born, D.A., Edwards, A., Gehrke, J.M., Lee, S.J., Liquori, A.J., et al. (2020). Directed evolution of

adenine base editors with increased activity and therapeutic application. Nature Biotechnology *38*, 892–900. https://doi.org/10.1038/s41587-020-0491-6.

40. Selvaraj, S., Feist, W.N., Viel, S., Vaidyanathan, S., Dudek, A.M., Gastou, M., Rockwood, S.J., Ekman, F.K., Oseghale, A.R., Xu, L., et al. (2024). High-efficiency transgene integration by homology-directed repair in human primary cells using DNA-PKcs inhibition. Nat Biotechnol *42*, 731–744. https://doi.org/10.1038/s41587-023-01888-4.

41. Glaser, V., Flugel, C., Kath, J., Du, W., Drosdek, V., Franke, C., Stein, M., Pruß, A., Schmueck-Henneresse, M., Volk, H.-D., et al. (2023). Combining different CRISPR nucleases for simultaneous knock-in and base editing prevents translocations in multiplex-edited CAR T cells. Genome Biol *24*, 89. https://doi.org/10.1186/s13059-023-02928-7.

42. Hsu, P.D., Scott, D.A., Weinstein, J.A., Ran, F.A., Konermann, S., Agarwala, V., Li, Y., Fine, E.J., Wu, X., Shalem, O., et al. (2013). DNA targeting specificity of RNA-guided Cas9 nucleases. Nat Biotechnol *31*, 827–832. https://doi.org/10.1038/nbt.2647.

43. Skeate, J.G., Slipek, N.J., Lahr, W.S., Roy, S., Wick, B.J., Stelljes, E.M., Gilkey, A.K., Thenge, P.P., Diers, M.D., Kar, B., et al. (2025). A Singular Base Editing Platform for Polyfunctional Multiplex Engineering of Immune Cells. Preprint at Cold Spring Harbor Laboratory, https://doi.org/10.1101/2025.07.11.664404 https://doi.org/10.1101/2025.07.11.664404.

44. Senes, A., Engel, D.E., and DeGrado, W.F. (2004). Folding of helical membrane proteins: the role of polar, GxxxG-like and proline motifs. Current Opinion in Structural Biology *14*, 465–479. https://doi.org/10.1016/j.sbi.2004.07.007.

45. Wang, D., Tai, P.W.L., and Gao, G. (2019). Adeno-associated virus vector as a platform for gene therapy delivery. Nat Rev Drug Discov *18*, 358–378. https://doi.org/10.1038/s41573-019-0012-9.

46. Wang, J.-H., Gessler, D.J., Zhan, W., Gallagher, T.L., and Gao, G. (2024). Adeno-associated virus as a delivery vector for gene therapy of human diseases. Sig Transduct Target Ther *9*, 78. https://doi.org/10.1038/s41392-024-01780-w.

47. Grünewald, J., Zhou, R., Garcia, S.P., Iyer, S., Lareau, C.A., Aryee, M.J., and Joung, J.K. (2019). Transcriptome-wide off-target RNA editing induced by CRISPR-guided DNA base editors. Nature *569*, 433–437. https://doi.org/10.1038/s41586-019-1161-z.

48. Garaudé, S., Marone, R., Lepore, R., Devaux, A., Beerlage, A., Seyres, D., Dell' Aglio, A., Juskevicius, D., Zuin, J., Burgold, T., et al. (2024). Selective haematological cancer eradication with preserved haematopoiesis. Nature *630*, 728–735. https://doi.org/10.1038/s41586-024-07456-3.

49. Kath, J., Du, W., Martini, S., Elsallab, M., Franke, C., Hartmann, L., Drosdek, V., Glaser, V., Stein, M., Schmueck-Henneresse, M., et al. (2023). CAR NK-92 cell–mediated depletion of residual TCR+ cells for ultrapure allogeneic TCR-deleted CAR

T-cell products. Blood Advances *7*, 4124–4134. https://doi.org/10.1182/bloodadvances.2022009397.

50. Diorio, C., Murray, R., Naniong, M., and et al (2022). Cytosine Base Editing Enables Quadruple-Edited Allogeneic CAR-T Cells for T-ALL. Blood.

51. Engel, N.W., Steinfeld, I., Ryan, D., Anupindi, K., Kim, S., Wellhausen, N., Chen, L., Wilkins, K., Baker, D.J., Rommel, P.C., et al. (2025). Quadruple adenine base-edited allogeneic CAR T cells outperform CRISPR/Cas9 nuclease-engineered T cells. Proc Natl Acad Sci U S A *122*, e2427216122. https://doi.org/10.1073/pnas.2427216122.

52. Engel, N.W., Steinfeld, I., Ryan, D., Anupindi, K., Kim, S., Wellhausen, N., Chen, L., Wilkins, K., Baker, D.J., Rommel, P.C., et al. (2025). Quadruple adenine base–edited allogeneic CAR T cells outperform CRISPR/Cas9 nuclease–engineered T cells. Proc. Natl. Acad. Sci. U.S.A. *122*. https://doi.org/10.1073/pnas.2427216122.

53. Jiang, L., Ingelshed, K., Shen, Y., Boddul, S.V., Iyer, V.S., Kasza, Z., Sedimbi, S., Lane, D.P., and Wermeling, F. (2022). CRISPR/Cas9-Induced DNA Damage Enriches for Mutations in a p53-Linked Interactome: Implications for CRISPR-Based Therapies. Cancer Research *82*, 36–45. https://doi.org/10.1158/0008-5472.CAN-21-1692.

54. Haapaniemi, E., Botla, S., Persson, J., Schmierer, B., and Taipale, J. (2018). CRISPR–Cas9 genome editing induces a p53-mediated DNA damage response. Nat Med *24*, 927–930. https://doi.org/10.1038/s41591-018-0049-z.

55. Georgiadis, C., Rasaiyaah, J., Gkazi, S.A., Preece, R., Etuk, A., Christi, A., and Qasim, W. (2021). Base-edited CAR T cells for combinational therapy against T cell malignancies. Leukemia *35*, 3466–3481. https://doi.org/10.1038/s41375-021-01282-6.

56. Wang, M., Krueger, J.B., Gilkey, A.K., Stelljes, E.M., Kluesner, M.G., Pomeroy, E.J., Skeate, J.G., Slipek, N.J., Lahr, W.S., Claudio Vázquez, P.N., et al. (2025). Precision enhancement of CAR-NK cells through non-viral engineering and highly multiplexed base editing. J Immunother Cancer *13*, e009560. https://doi.org/10.1136/jitc-2024-009560.

57. Harrison, S.J., Touzeau, C., Kint, N., Li, K., Nguyen, T., Mayeur-Rousse, C., Rahman, M., Le Bris, Y., Er, J., Eugene-Lamer, J., et al. (2025). CAR+ T-Cell Lymphoma after Cilta-cel Therapy for Relapsed or Refractory Myeloma. N Engl J Med *392*, 677–685. https://doi.org/10.1056/nejmoa2309728.

58. Elsallab, M., Ellithi, M., Lunning, M.A., D'Angelo, C., Ma, J., Perales, M.-A., Frigault, M., and Maus, M.V. (2024). Second primary malignancies after commercial CAR T-cell therapy: analysis of the FDA Adverse Events Reporting System. Blood *143*, 2099–2105. https://doi.org/10.1182/blood.2024024166.

59. Jo, S., Das, S., Williams, A., Chretien, A.-S., Pagliardini, T., Le Roy, A., Fernandez, J.P., Le Clerre, D., Jahangiri, B., Chion-Sotinel, I., et al. (2022). Endowing universal CAR T-cell with immune-evasive properties using TALEN-gene editing. Nat Commun *13*, 3453. https://doi.org/10.1038/s41467-022-30896-2.

60. Chang, C.R., Vykunta, V.S., Lee, J.H.J., Li, K., Kochendoerfer, C., Muldoon, J.J., Wang, C.H., Mazumder, T., Sun, Y., Goodman, D.B., et al. (2025). SEED-Selection enables high-efficiency enrichment of primary T cells edited at multiple loci. Nat Biotechnol. https://doi.org/10.1038/s41587-024-02531-6.

61. Allen, A.G., Khan, S.Q., Margulies, C.M., Viswanathan, R., Lele, S., Blaha, L., Scott, S.N., Izzo, K.M., Gerew, A., Pattali, R., et al. (2024). A highly efficient transgene knock-in technology in clinically relevant cell types. Nat Biotechnol *42*, 458–469. https://doi.org/10.1038/s41587-023-01779-8.

62. Porreca, I., Blassberg, R., Harbottle, J., Joubert, B., Mielczarek, O., Stombaugh, J., Hemphill, K., Sumner, J., Pazeraitis, D., Touza, J.L., et al. (2024). An aptamer-mediated base editing platform for simultaneous knockin and multiple gene knockout for allogeneic CAR-T cells generation. Molecular Therapy *32*, 2692–2710. https://doi.org/10.1016/j.ymthe.2024.06.033.

63. Foss, D.V., Muldoon, J.J., Nguyen, D.N., Carr, D., Sahu, S.U., Hunsinger, J.M., Wyman, S.K., Krishnappa, N., Mendonsa, R., Schanzer, E.V., et al. (2023). Peptide-mediated delivery of CRISPR enzymes for the efficient editing of primary human lymphocytes. Nat. Biomed. Eng *7*, 647–660. https://doi.org/10.1038/s41551-023-01032-2.

64. Kitte, R., Rabel, M., Geczy, R., Park, S., Fricke, S., Koehl, U., and Tretbar, U.S. (2023). Lipid nanoparticles outperform electroporation in mRNA-based CAR T cell engineering. Molecular Therapy - Methods & Clinical Development *31*, 101139. https://doi.org/10.1016/j.omtm.2023.101139.

65. Anzalone, A.V., Gao, X.D., Podracky, C.J., Nelson, A.T., Koblan, L.W., Raguram, A., Levy, J.M., Mercer, J.A.M., and Liu, D.R. (2022). Programmable deletion, replacement, integration and inversion of large DNA sequences with twin prime editing. Nat Biotechnol *40*, 731–740. https://doi.org/10.1038/s41587-021-01133-w.

66. Yarnall, M.T.N., Ioannidi, E.I., Schmitt-Ulms, C., Krajeski, R.N., Lim, J., Villiger, L., Zhou, W., Jiang, K., Garushyants, S.K., Roberts, N., et al. (2023). Drag-and-drop genome insertion of large sequences without double-strand DNA cleavage using CRISPR-directed integrases. Nat Biotechnol *41*, 500–512. https://doi.org/10.1038/s41587-022-01527-4.

67. Witte, I.P., Lampe, G.D., Eitzinger, S., Miller, S.M., Berríos, K.N., McElroy, A.N., King, R.T., Stringham, O.G., Gelsinger, D.R., Vo, P.L.H., et al. (2025). Programmable gene insertion in human cells with a laboratory-evolved CRISPR-associated transposase. Science *388*, eadt5199. https://doi.org/10.1126/science.adt5199.

68. Kassing, I., Kath, J., Nitulescu, A.-M., Glaser, V., Hartmann, L.M., Pu, Y., Huth, L., Kārkliņš, R., Shaji, S., Ringel, A.R., et al. (2025). Versatile and efficient non-viral integration of large transgenes in human T cells via CRISPR knock-in and engineered integrases. Preprint at Synthetic Biology, https://doi.org/10.1101/2025.09.10.675267 https://doi.org/10.1101/2025.09.10.675267.

69. Yu, Y., Leete, T.C., Born, D.A., Young, L., Barrera, L.A., Lee, S.-J., Rees, H.A., Ciaramella, G., and Gaudelli, N.M. (2020). Cytosine base editors with minimized unguided DNA and RNA off-target events and high on-target activity. Nat Commun *11*, 2052. https://doi.org/10.1038/s41467-020-15887-5.

70. Walsh, Z.H., Shah, P., Kothapalli, N., Shah, S.B., Nikolenyi, G., Brodtman, D.Z., Leuzzi, G., Rogava, M., Mu, M., Ho, P., et al. (2025). Mapping variant effects on anti-tumor hallmarks of primary human T cells with base-editing screens. Nat Biotechnol *43*, 384–395. https://doi.org/10.1038/s41587-024-02235-x.

71. Schmidt, R., Ward, C.C., Dajani, R., Armour-Garb, Z., Ota, M., Allain, V., Hernandez, R., Layeghi, M., Xing, G., Goudy, L., et al. (2024). Base-editing mutagenesis maps alleles to tune human T cell functions. Nature *625*, 805–812. https://doi.org/10.1038/s41586-023-06835-6.

72. Cradick, T.J., Qiu, P., Lee, C.M., Fine, E.J., and Bao, G. (2014). COSMID: A web-based tool for identifying and validating CRISPR/Cas off-target sites. Molecular Therapy - Nucleic Acids *3*, e214. https://doi.org/10.1038/mtna.2014.64.

73. Ye, J., Coulouris, G., Zaretskaya, I., Cutcutache, I., Rozen, S., and Madden, T.L. (2012). Primer-BLAST: A tool to design target-specific primers for polymerase chain reaction. BMC Bioinformatics *13*, 134. https://doi.org/10.1186/1471-2105-13-134.

74. Kluesner, M.G., Nedveck, D.A., Lahr, W.S., Garbe, J.R., Abrahante, J.E., Webber, B.R., and Moriarity, B.S. (2018). EditR: A Method to Quantify Base Editing from Sanger Sequencing. The CRISPR Journal *1*, 239–250. https://doi.org/10.1089/crispr.2018.0014.

75. Conant, D., Hsiau, T., Rossi, N., Oki, J., Maures, T., Waite, K., Yang, J., Joshi, S., Kelso, R., Holden, K., et al. (2022). Inference of CRISPR Edits from Sanger Trace Data. The CRISPR Journal *5*, 123–130. https://doi.org/10.1089/crispr.2021.0113.

76. Turchiano, G., Andrieux, G., Klermund, J., Blattner, G., Pennucci, V., El Gaz, M., Monaco, G., Poddar, S., Mussolino, C., Cornu, T.I., et al. (2021). Quantitative evaluation of chromosomal rearrangements in gene-edited human stem cells by CAST-Seq. Cell Stem Cell *28*, 1136-1147.e5. https://doi.org/10.1016/j.stem.2021.02.002.

77. Rhiel, M., Geiger, K., Andrieux, G., Rositzka, J., Boerries, M., Cathomen, T., and Cornu, T.I. (2023). T-CAST: An optimized CAST-Seq pipeline for TALEN confirms superior safety and efficacy of obligate-heterodimeric scaffolds. Front. Genome Ed. *5*, 1130736. https://doi.org/10.3389/fgeed.2023.1130736.

List of Figure Legends

Fig. 1 | sgRNA pair design for site-specific integration of CAR transgenes using a double nick approach with nCas9 or base editors. (**A**) Schematic overview of the double nick strategy for the insertion of a second generation CD19 CAR into the *TRAC* locus and the location and direction of the 12 sgRNAs used. (**B**) Nick distance of the 36 sgRNA combinations targeting opposed DNA strands. Nick distances of PAM-in oriented sgRNA pairs are displayed as negative values. (**C**) KI-efficiency using a D10A nCas9 was evaluated on day 4 after electroporation via flow cytometry (n=2 healthy donors). The results are displayed as a heatmap corresponding to B) and as a graph plotting the KI rate against the nick distance. (**D**) KI-efficiency using ABE8.20-m was evaluated on day 4 after electroporation via flow cytometry (n=2 healthy donors). The results are displayed as a heatmap corresponding to B) and as a graph plotting the KI rate against the nick distance. (**E**) KI-efficiency using a CBE (BE4) were evaluated on day 4 after electroporation via flow cytometry (n=2 healthy donors). The results are displayed as a heatmap corresponding to B) and as a graph plotting the KI rate against the nick distance.

Fig. 2 | BEKI enables efficient gene editing at multiple therapeutically relevant loci. (**A**) Schematic overview of the double nick strategy for the insertion of a truncated (trunc)CD19 CAR into the *CD3ζ* locus and the location and direction of the 8 sgRNAs evaluated. Heatmaps are showing the nick distance of the 16 sgRNA combinations targeting opposed DNA strands and the KI-efficiency using ABE8.20-m, evaluated on day 4 after electroporation via flow cytometry (n=4 healthy donors). (**B**) The same was displayed for the KI of HLA-E into the *B2M* locus (8 sgRNAs, n=2) and (**C**) a CD19-specific TRuC into *CD3ε* (5 sgRNAs, n=3 healthy donors). (**D**) The KI-rate was

normalized to the most efficient KI for each of the 4 tested loci (color) and plotted against the nick distance. The window for optimal editing was manually added. (**E**) The normalized KI-rate of editing at the 4 tested loci (color) was plotted against the number of adenines (A) in the editing window (5 and 6 As (n=1) are not shown) (**F**) The normalized KI-rate (circle size) of 4 tested loci (color) was plotted against the number of adenines (A) in the editing window and the nick distance.

Fig. 3 | HDR enhancers improve BEKI editing efficiency and enable potent in vivo activity of CD19 CAR T cells. (**A**) Efficiency of ABE-mediated KI of a CD19-specific truncCAR into *CD3ζ* without HDR enhancers. Z1 was excluded for this experiment due to low initial KI-rates (n=2 healthy donors). ABE-mediated KI-efficiency of a CD19 truncCAR into *CD3ζ* with DNA PK inhibitor AZD7648 (2μM) and Polθ inhibitor novobiocin (10μM); (n=2 healthy donors). Representative flow cytometry histograms show different editing outcomes when adding DNA PK and Polθ inhibitors. KI-rate of the most efficient combination for *CD3ζ* KI using ABE: Z4+Z7 (n=2 healthy donors). (**B**) CBE-mediated KI-efficiency of a CD19 truncCAR into *CD3ζ* without HDR enhancers (n=2-6 healthy donors). CBE-mediated KI-efficiency of a CD19 truncCAR into *CD3ζ* with DNA PK and Polθ inhibitors AZD7648 and ART558 (n=2-6 healthy donors). Representative flow cytometry histograms show different editing outcomes when adding DNA PK and Polθ inhibitors. KI-rate of the most efficient combination for *CD3ζ* KI using CBE: Z4+Z8 (n=4 healthy donors). (**C**) Schematic overview of an acute lymphoblastic leukemia xenograft mouse model using luciferase-labeled Nalm6 (CD19+) tumor cells. 7 days post Nalm6 administration, 0.5×10^6 cryopreserved CAR+ T cells were injected systemically. A blood sample was taken from all mice on day 28 after injection of the Nalm6 tumor cells. Flow cytometric analysis was performed to

quantify the frequency of GFP+ Nalm6 cells. Additionally, tumor burden was assessed via bioluminescence imaging (n = 5 mice). A multiple unpaired T test using the two-stage step-up method (Benjamini, Krieger, and Yekutieli) of log-transformed bioluminescence imaging data. Asterisks represent the following p-values: (ns: $p \geq 0.05$; *: $p < 0.05$; **: $p < 0.01$; ***: $p < 0.001$).

Fig. 4 | ART558 and DNA templates limit large deletions caused by AZD7648 (**A**) Schematic of long-read Oxford Nanopore Technologies (ONT) sequencing strategy for the *TRAC* locus. (**B, C**) Quantification by long-read sequencing of the fraction of total reads with a length greater than a defined size and quantified frequency of deletions larger than 2 kb or 1 kb in edited T cells. (**D**) Schematic representation of droplet digital PCR (ddPCR) assays designed to detect megabase-scale deletions. (**E**) Average fold change in copy number measured by the *ZHFX2* ddPCR assay relative to the *KM2TC* reference assay in mock-treated and Cas9-treated T cells in the absence of donor DNA template. (**F**) Average fold change in *ZHFX2* relative to *KM2TC* in gene-edited T cells cultured with or without enhancer treatment. Data are from n = 2 biological replicates.

Fig. 5 | BEKI minimizes chromosomal translocations during simultaneous knock-in and multi-gene knockout. (**A**) Schematic overview of the different gene editing strategies targeting the *TRAC, RASA2* and *FKBP12* gene to create cells with (I) *TRF* KO using Cas9, (II) CAR KI + *TRF* KO using Cas9, (III) CAR KI + *TRF* KO using Cas12a for the KI and ABE for the *RF* KO and (IV) CAR KI + *TRF* KO using ABE. (**B**) Gene editing efficiency of CAR KI and *TRAC* KO (CD3 staining) was determined by flow cytometry. KO- or BE-efficiency of *RASA2* and *FKBP12* gene were assessed using Sanger sequencing followed by indel analysis using ICE CRISPR analysis. 2025.

v3.0. (EditCo Bio) or base editing frequency via EditR. (**C**) Circos plot shows results of chromosomal rearrangements detected in cells edited with Cas9, Cas12a + ABE or ABE using CAST-Seq (excluding an HDR donor template). On-target (ON) genomic aberrations are indicated in green (*TRAC*) or purple (*RASA2, FKBP12*), and off-target mediated rearrangement between the *TRAC* target site and off-target (OMT) site in red. The color intensity of the arcs directly reflect the relative frequency of translocations, normalized to the most frequent event, with the corresponding range indicated in the heatmap legend on the right. (**D**) Frequencies of balanced translocations between the on-target genes were determined by ddPCR. They are shown for all six individual translocations and as the sum of all translocations detected in mock, (I) TRF KO (Cas9) or CAR KI + TRF KO ((II) Cas9, (III) Cas12a+ABE, (IV) ABE) conditions (n = 3 healthy donors). Statistical analysis of ddPCR was performed using a one-way ANOVA of matched data with Geisser-Greenhouse correction. Multiple comparisons were performed by comparing the mean of each column with the mean of every other column and corrected by the Tukey test. Asterisks represent the following p-values: (ns: $p \geq 0.05$; *: $p < 0.05$; **: $p < 0.01$; ***: $p < 0.001$).

Fig. 6 | BEKI enables efficient multiplexed editing for combining CAR KI with up to 10 KOs

(**A**) Schematic overview of genomic targets for base editing-mediated KO that could improve *CD3ζ* CAR. (**B**) Gene editing efficiency was evaluated using flow cytometry for CAR KI into *CD3ζ,* as well as well as relative loss of surface protein expression of CD3 normalized to mock and HLA-I, HLA-II, CD54, CD58, CD2, CD5, CD7, CD38, Fas and CD45 normalized to the CAR only control (n = 2 healthy donors). Relative loss of surface protein expression was calculated as 100 – (target positive in gene-edited condition/target positive in control × 100).

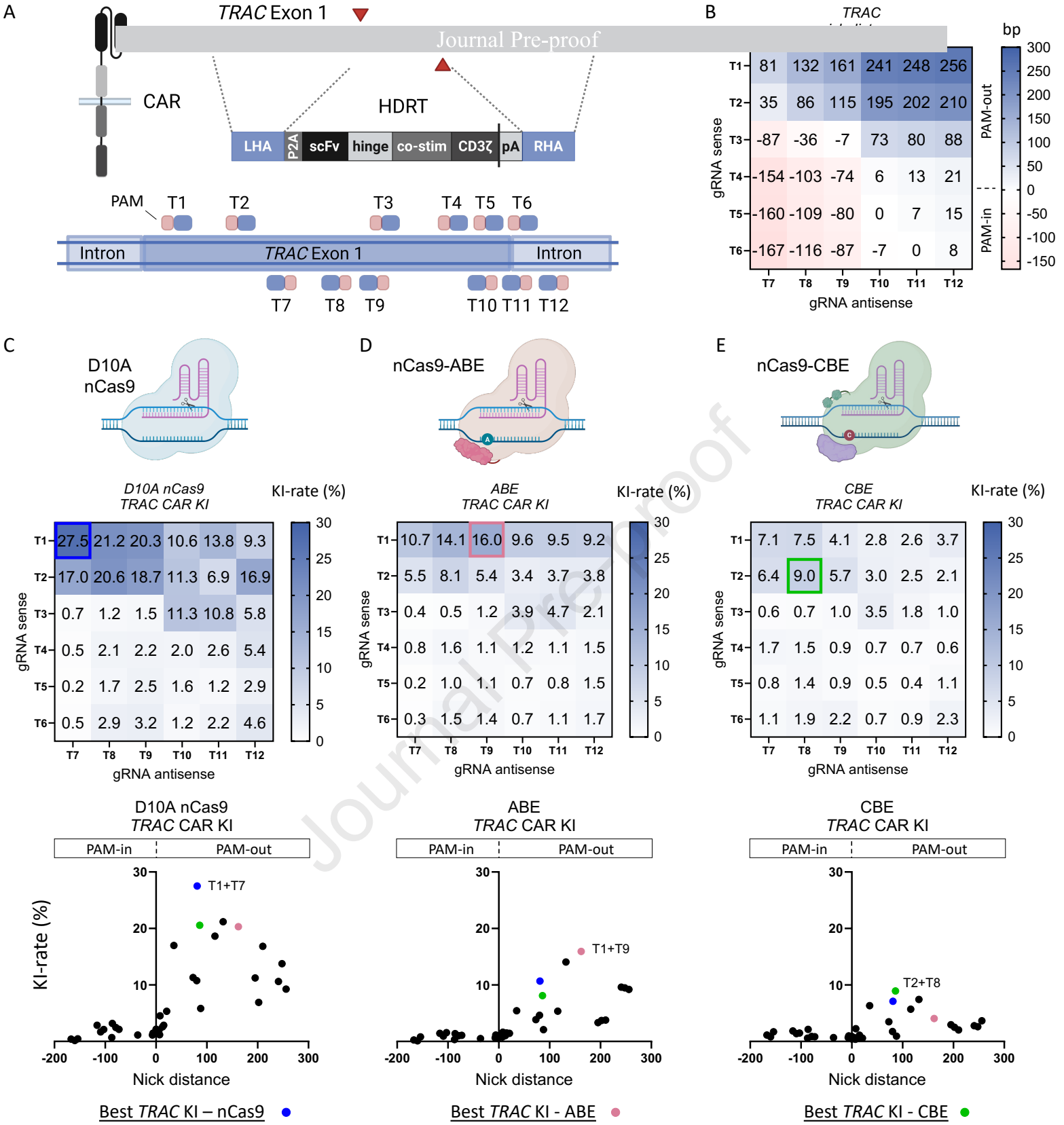

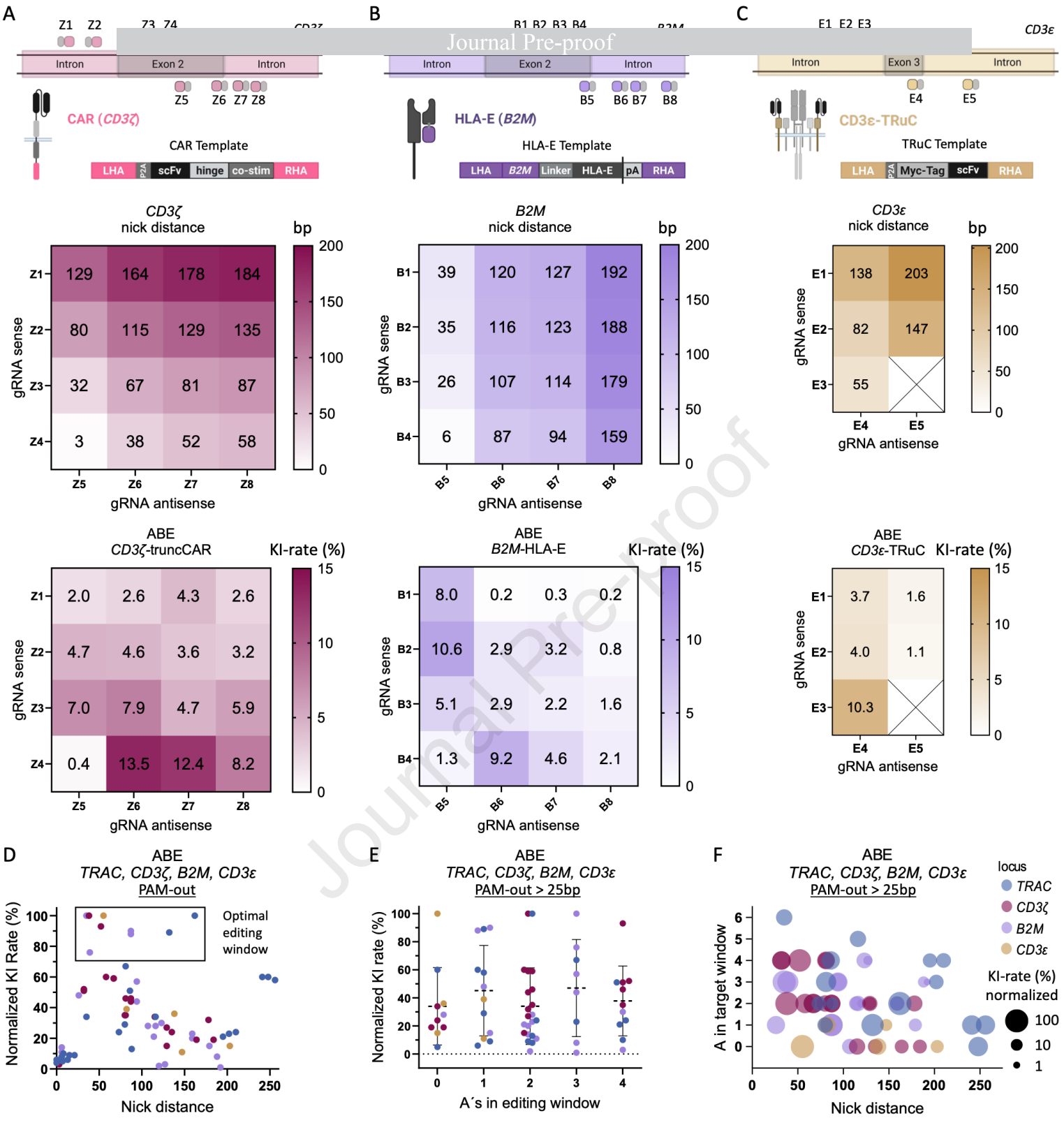

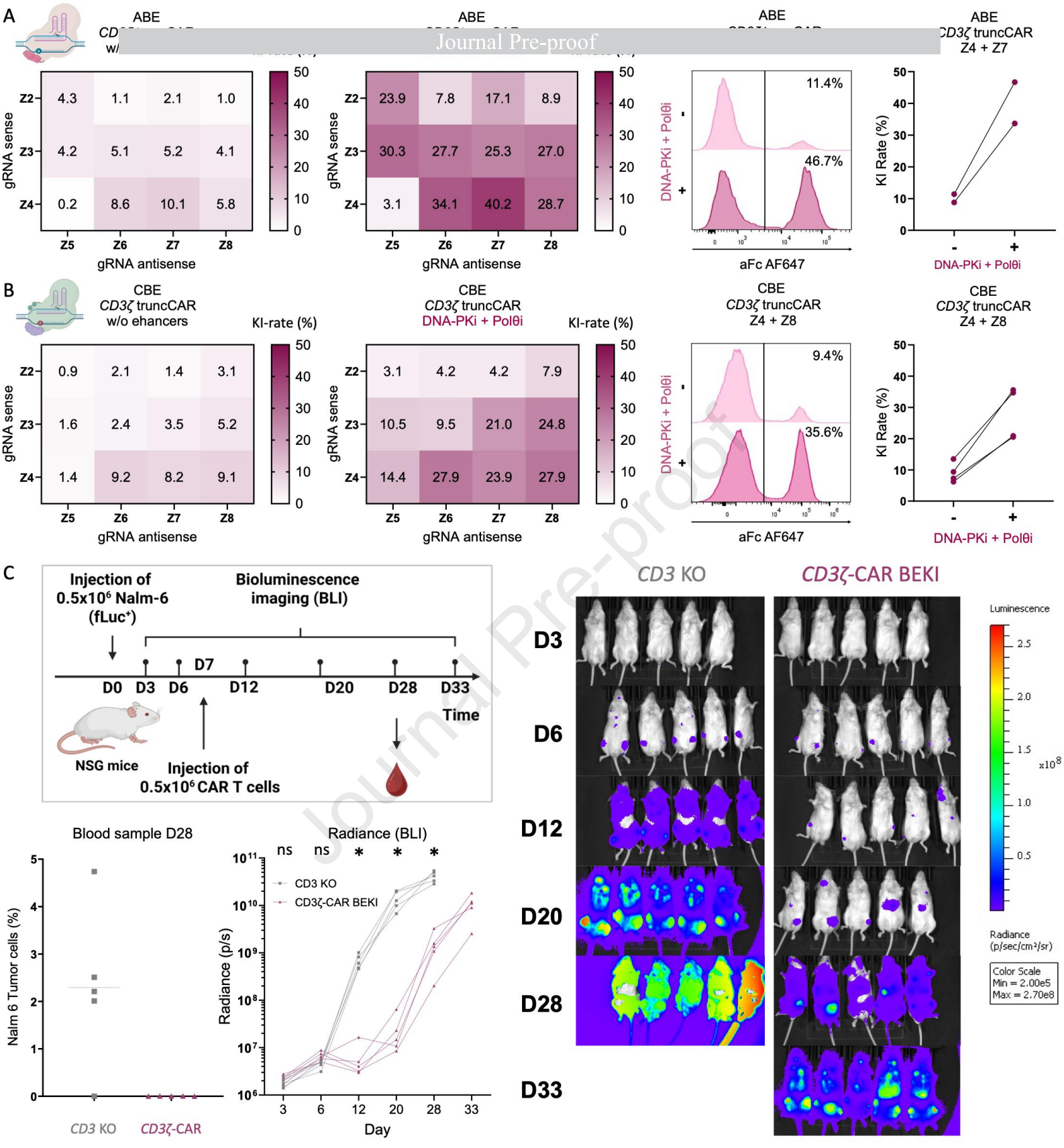

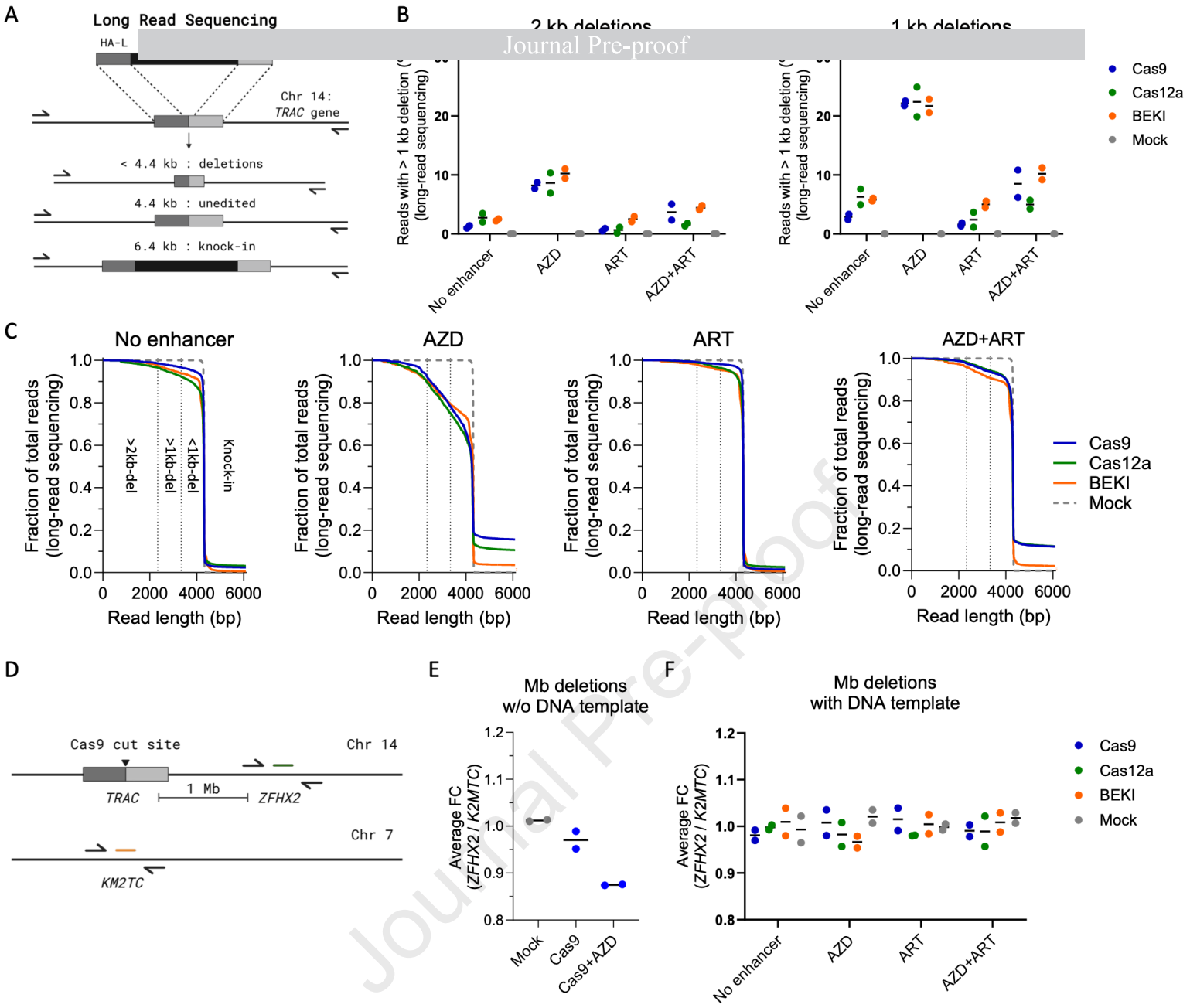

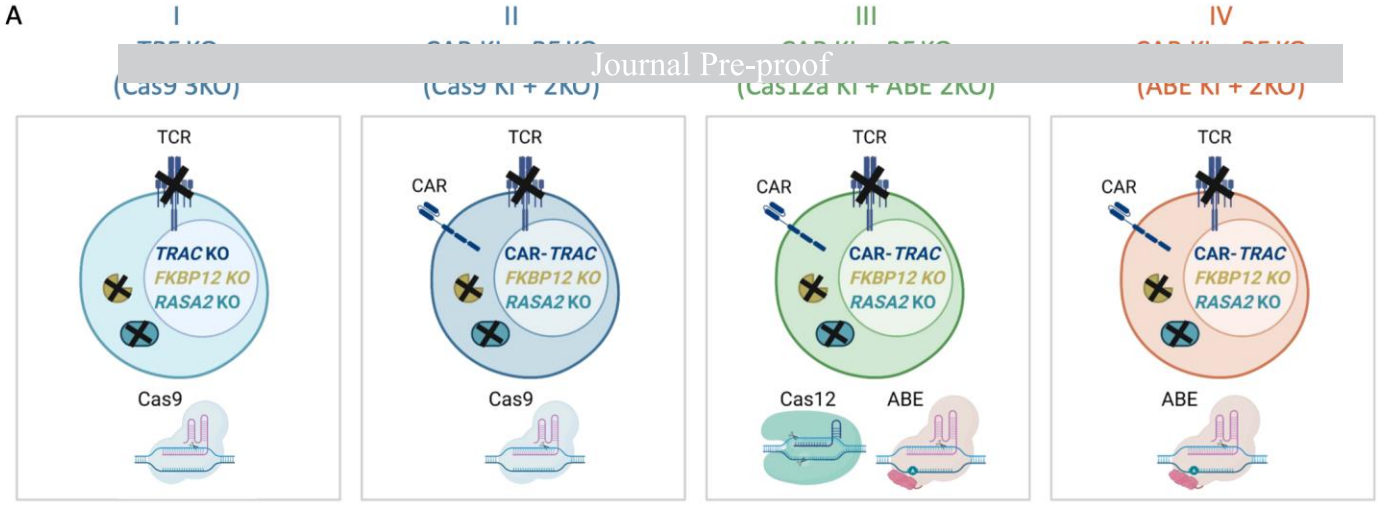

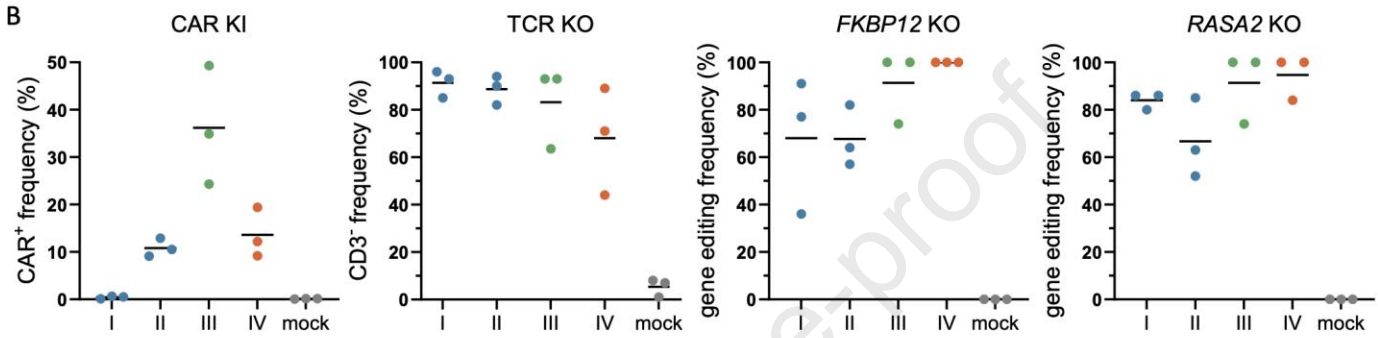

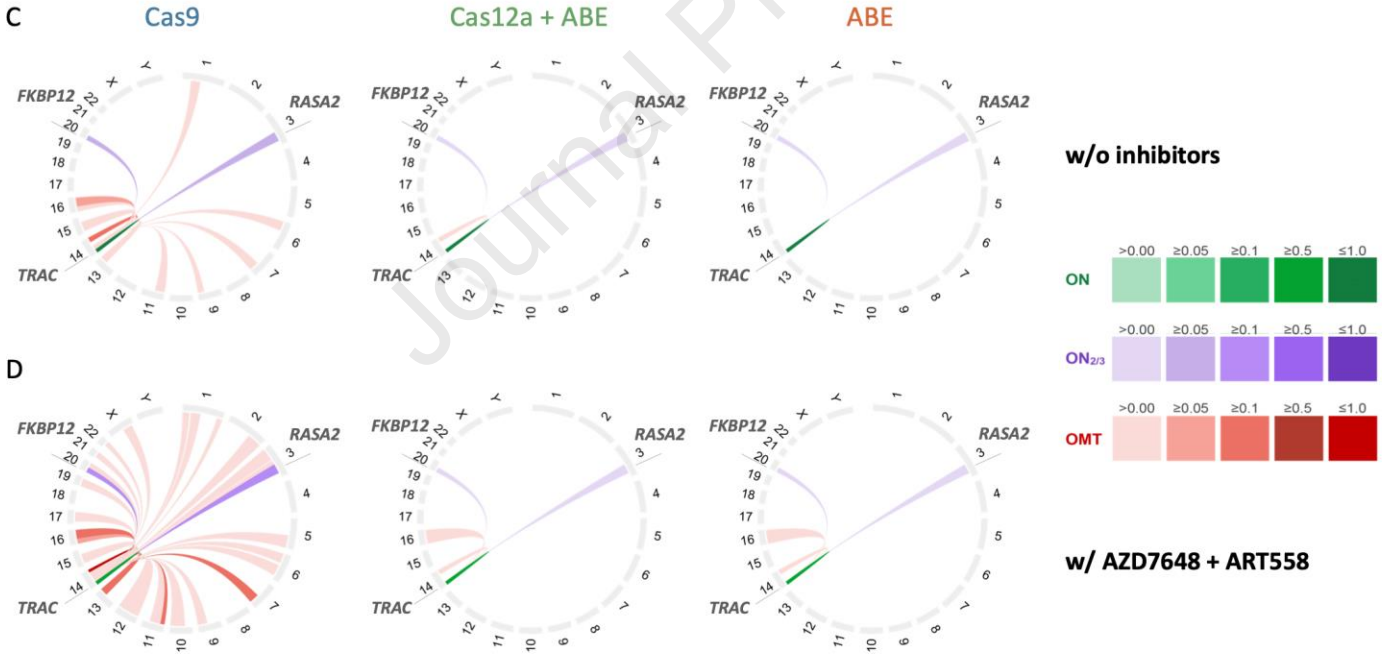

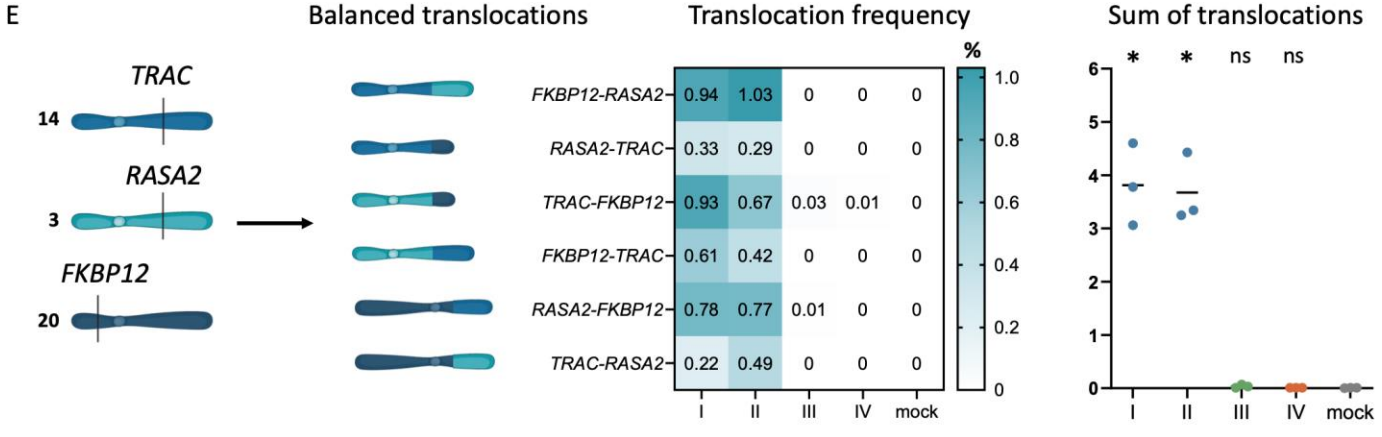

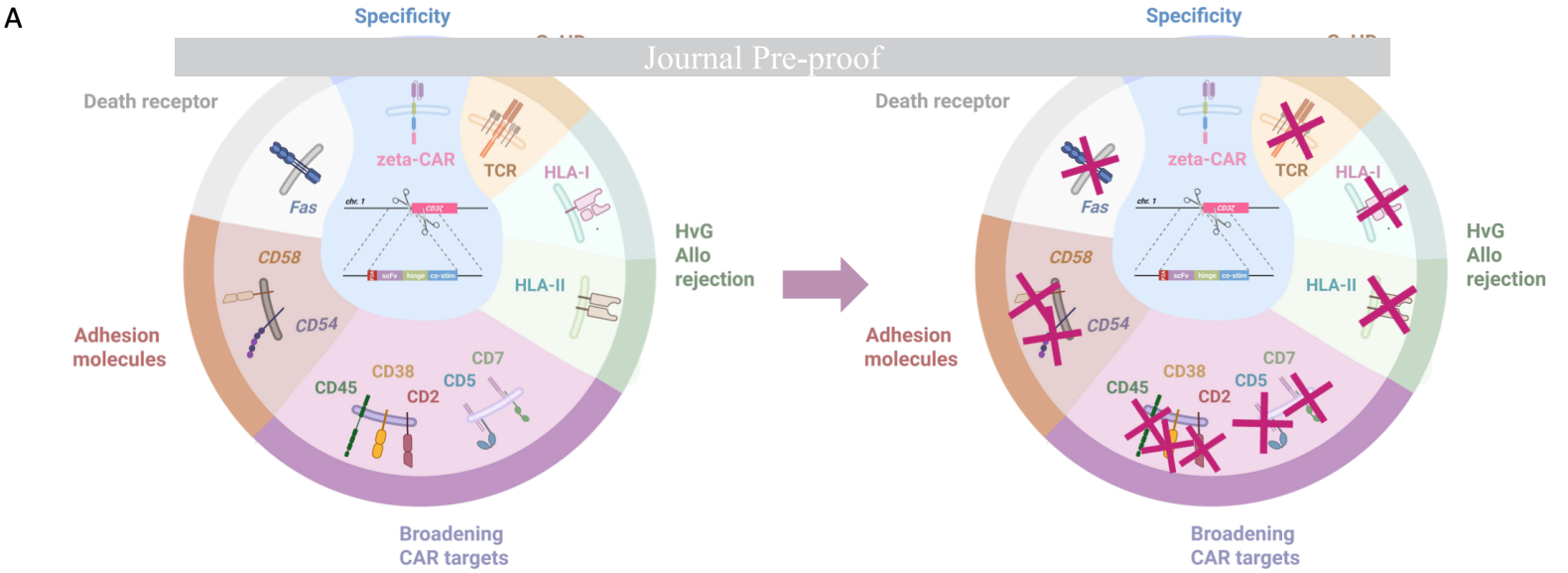

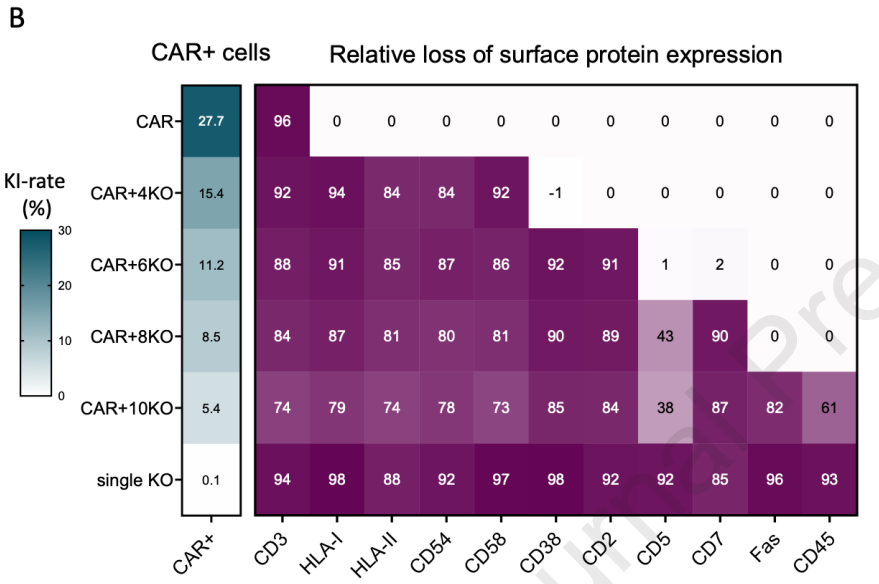

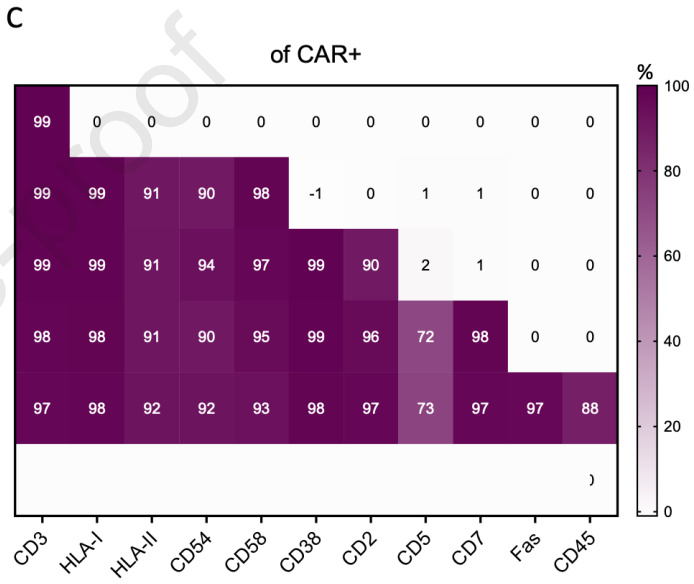

Wagner and colleagues develop BEKI (Base Editor-mediated Knock-In), a non-viral platform that combines targeted transgene insertion with simultaneous gene knockouts in a single step. BEKI-engineered CAR T cells show markedly reduced chromosomal rearrangements compared to conventional nuclease-based approaches, advancing safer manufacturing of multiplex-edited cell therapies for cancer and autoimmune diseases.